TRAP1 AND THE PROTEASOME REGULATORY PARTICLE TBP7/Rpt3 INTERACT IN THE ENDOPLASMIC RETICULUM AND CONTROL CELLULAR UBIQUITINATION OF SPECIFIC MITOCHONDRIAL PROTEINS

Franca Esposito, Maria Rosaria Amoroso, Danilo Swann Matassa, Gabriella Laudiero, Anastasia Egorova, Roman Polishchuk, Francesca Maddalena, Annamaria Piscazzi, Corrado Garbi, Matteo Landriscina, et al.

TRAP1 AND THE PROTEASOME REGULATORY PARTICLE TBP7/Rpt3 INTERACT IN THE ENDOPLASMIC RETICULUM AND CONTROL CELLULAR UBIQUITINATION OF SPECIFIC MITOCHONDRIAL PROTEINS

Running Title: TRAP1/TBP7 network in protein quality control.

Maria Rosaria Amoroso[1], Danilo Swann Matassa[1], Gabriella Laudiero[1], Anastasia V. Egorova[2], Roman S. Polishchuk[2], Francesca Maddalena[3], Annamaria Piscazzi[4], Simona Paladino[5,6], Daniela Sarnataro[5,6], Corrado Garbi[5], Matteo Landriscina[4] and Franca Esposito[1]

[1]Department of Biochemistry and Medical Biotechnologies, University of Naples Federico II, Via Pansini 5, 80131, Naples, Italy, [2]Telethon Institute of Genetics and Medicine (TIGEM), Via Pietro Castellino 111, 80131, Naples, Italy; [3]IRCCS CROB, Rionero in Vulture, Italy; [4]Clinical Oncology Unit, Department of Medical Sciences, University of Foggia, Foggia, Italy; [5]Department of Biology and Molecular and Cellular Pathology, University of Naples Federico II, Naples, Italy; [6]CEINGE Biotecnologie Avanzate S.C.A.R.L., Naples, Italy.

Corresponding authors

Prof. Franca Esposito, Dipartimento di Biochimica e Biotecnologie Mediche, Università di Napoli Federico II, Via Pansini 5 – 80131, Napoli, Italy. Phone: +39 081 7463145; Fax: +39 081 7464359; E-mail: franca.esposito@unina.it

Dr. Matteo Landriscina, Dipartimento di Scienze Mediche e del Lavoro, Università degli Studi di Foggia, Viale Pinto, 1 – 71100 Foggia, Italy. Phone: +39 0881 736241; Fax: +39 0881 733614; E-mail: m.landriscina@unifg.it

ABSTRACT

TRAP1 is a mitochondrial antiapoptotic heat shock protein. The information available on the TRAP1 pathway describes just a few well-characterized functions of this protein in mitochondria. However, our group's use of mass spectrometry analysis identified TBP7, an AAA-ATPase of the 19S proteasomal subunit, as a putative TRAP1-interacting protein. Surprisingly, TRAP1 and TBP7 co-localize in the endoplasmic reticulum (ER), as demonstrated by biochemical and confocal/electron microscopy analyses, and directly interact, as confirmed by FRET analysis. This is the first demonstration of TRAP1 presence in this cellular compartment. TRAP1 silencing by shRNAs, in cells exposed to thapsigargin-induced ER stress, correlates with up-regulation of BiP/ Grp78, thus suggesting a role of TRAP1 in the refolding of damaged proteins and in ER stress protection. Consistently, TRAP1 and/or TBP7 interference enhanced stress-induced cell death and increased intracellular protein ubiquitination. These experiments led us to hypothesize an involvement of TRAP1 in protein quality control for mistargeted/misfolded mitochondria-destined proteins, through interaction with the regulatory proteasome protein TBP7. Remarkably, the expression of specific mitochondrial proteins decreased upon TRAP1 interference as a consequence of increased ubiquitination. The proposed TRAP1 network has an impact *in vivo*, since it is conserved in human colorectal cancers, is controlled by ER-localized TRAP1 interacting with TBP7 and provides a novel model of ER-mitochondria crosstalk.

Keywords: TRAP1, TBP7, mitochondria/ER crosstalk, protein quality control, ubiquitination, apoptosis

INTRODUCTION

Tumor necrosis factor receptor-associated protein 1 (TRAP1) was initially identified as TNF-receptor-associated protein and is a member of the heat shock protein 90 (HSP90) chaperone family (1, 2). Through a mRNA-differential display analysis between oxidant-adapted and control osteosarcoma cells, our group identified, among other proteins, TRAP1 whose expression was highly induced upon oxidant adaptation (3). Furthermore, TRAP1 exhibited antioxidant and antiapoptotic functions (4), while an involvement of this mitochondrial chaperone in the multi-drug resistance of human colorectal carcinoma (CRC) cells was also established (5).

Little is known about TRAP1 signal transduction: the first most important finding on TRAP1 function came in studies by the Altieri's group that identified TRAP1 as a member of a cytoprotective network selectively active in the mitochondria of tumor tissues (6). The same group has recently proposed TRAP1 as a novel molecular target in localized and metastatic prostate cancer (7) and is now involved in a promising preclinical characterization of mitochondria-targeted small molecule HSP90 inhibitors (8, 9). Besides some well-characterized TRAP1 functions in mitochondria, during preparation of this manuscript it was reported that HSP90 chaperones interference triggers an unfolded protein response (UPR) and activates autophagy in mitochondria of tumor cells (10). A putative role of TRAP1 in endoplasmic reticulum (ER) stress control was concomitantly suggested by Takemoto et al. (11), even though no evidence as to the mechanisms involved was provided in this study.

A proteomic analysis of TRAP1 co-immunoprecipitation complexes was performed in our laboratory, in order to further characterize the TRAP1 network and evaluate protein interactors relevant for its roles. Among several other proteins, a novel mitochondrial isoform of Sorcin, a calcium-binding protein, was identified as a new TRAP1 "ligand" and a cytoprotective function against apoptosis induced by antiblastic agents was recently demonstrated for this protein by our group (12). In the present article, we characterize another new interaction of TRAP1 with TBP7/ATPase 4/Rpt3, a S6 ATPase protein of the proteasome regulatory subunit. TBP7 was firstly

identified as a novel synphilin-1 interacting protein (13), so a functional role in Parkinson's disease was proposed for this protein. However, not many novel results became available subsequently on TBP7 function. It is known that the 26S proteasome is an enzymatic complex that degrades ubiquitinated proteins in eukaryotic cells. It is composed of the 20S core particle (CP) and the 19S regulatory particle (RP). While the mechanism involved in the assembly of the CP is well investigated, that of the RP is poorly understood (14).

Altogether, i) the absence of TBP7 in mitochondria, ii) its still uncharacterized function as a proteasome regulatory protein, and iii) its association with TRAP1 prompted us to analyze the sub-cellular localization of TRAP1/TBP7 interaction and to investigate its functional role. Several studies have described a function of HSP in the control of gene expression (15, 16) and recent evidence demonstrated the importance of 19S ATPases in the transcription machinery, as well as their additional regulatory mechanisms in mammalian transcription (17). Therefore, we hypothesized that TRAP1/TBP7 interaction might play a role in protein-quality control and cellular ubiquitination. Moreover, the finding that the two proteins directly interact in the ER further supports our hypothesis, since it is known that misfolding of proteins either emerging from or entering into the ER is tightly controlled by a large number of molecular chaperones and, if the quality control fails, they are ubiquitinated and degraded by the proteasome (18). This paper, for the first time, describes the presence of TRAP1 on the outer side of the ER and shows the functional role that TRAP1 plays in the quality control of proteins destined to mitochondria, and in the regulation of intracellular protein ubiquitination, through the interaction with TBP7.

RESULTS

TRAP1 and TBP7 colocalize and dierctly interact in the ER

The "fishing for partners" strategy combined with mass spectrometric procedures carried out to identify TRAP1 protein partners has already been described elsewhere (12).

Among the putative TRAP1 binding partners, we focused our attention on a protein of about 50 kDa identified by our LC-MS/MS analysis as S6/TBP7/ATPase 4/Rpt3 (19). To confirm that this proteasome subunit was indeed a TRAP1 interacting protein we performed western blot (WB) and co-immunoprecipitation (co-IP) analyses in total extracts from HCT116 colon carcinoma cells (Figure 1, Panel A). Since TRAP1 is localized in mitochondria, a subfractionation of HCT116 cellular extracts was performed. Surprisingly, WB analysis of sub-cellular compartments failed to demonstrate the presence of the proteasome regulatory protein in mitochondria, but identified TBP7 both in the cytosol and microsomal fraction (Figure 1, Panel B). Co-IP analyses from ER fraction confirmed TRAP1/TBP7 interaction in the ER (Figure 1, Panel C).

TRAP1/TBP7 molecular interaction was further investigated by using a fluorescence resonance energy transfer (FRET) approach in fixed cells (Figure 1, Panel D). Specifically we utilized the acceptor photobleaching technique where, upon irreversible photobleaching, the changes in the donor fluorescence were recorded (20). In cells co-expressing wild-types TRAP1 and TBP7 we found about 12% of FRET efficiency (Figure 1, panel D) indicating that TRAP1 and TBP7 are close enough to allow energy transfer. Interestingly we found FRET exclusively when we bleached ER regions, which we selected on the basis of their morphological features (one example in Figure 1, panel D, a-f). Thus, these data indicate that TRAP1 and TBP7 directly interact with each other and this interaction occurs specifically in the ER compartments. Furthermore, according to biochemical data described below in the manuscript (Supplementary Figure 1 and Figure 4, Panel H) we found no FRET between TRAP1 and a mutant form of TBP7 (Figure 1, panel D).

Since it had never been reported previously, we aimed to further confirm the novel localization of this mitochondrial chaperone in the ER through electron microscopy (EM) and confocal microscopy analyses (Figure 1, Panels E and F). To further evaluate whether TRAP1 is associated with the ER membranes, cells stably expressing TRAP-HA vectors were prepared for immuno-EM. Labeling with anti-HA antibody revealed significant amounts of TRAP1 in mitochondria (Figure 1, Panel E, a, b arrowheads), as has been previously reported (6). In addition, we found that TRAP1 was

distributed throughout the elongated membrane profiles (Figure 1, Panel E, a, arrows) that on the basis of their ultrastructural features (such as attached ribosomes) can be attributed to the rough ER compartment. Moreover, gold particles - indicating TRAP1 molecules - were detected along the nuclear envelope (Figure 1, Panel E, b, arrows), considered to be part of the ER membrane network. A careful examination of the density of immuno-gold labeling (in arbitrary units; average±SD) over different intracellular membranes allowed us to demonstrate that indeed, TRAP1 was enriched in mitochondria (2.53±0.34) as it has been already reported. However significant labeling density was also calculated for ER membranes (1.02±0.22) as shown in Figure 1, Panel E. Taken together, the EM observations are in line with the above results showing association of TRAP1 with the ER (Figure 1, Panels A-C). Accordingly, immunofluorescence confocal microscopy analysis showed TBP7 co-localization with TRAP1 and with the ER protein calnexin, thus further confirming ER localization (Figure 1, Panel F).

Altogether, these findings demonstrate that the interaction between TRAP1 and TBP7 occurs in the ER, but are unable to reveal a detailed localization in this context. To further evaluate the "topology" of TRAP1 and TBP7 in the ER, a biochemical assay based on protease digestion was performed. Figure 1, Panel G shows that both proteins are sensitive to a proteinase K digestion, while calnexin, a well-known ER-resident protein, is undigested. These approaches allowed us to demonstrate that TRAP1 and TBP7 are located on the outside of the ER. Moreover, alkaline treatment of ER fractions to remove peripheral membrane proteins allowed us to demonstrate that both TRAP1 and TBP7 are loosely associated to ER membranes (Figure 1 Panel H).

TRAP1 interference sensitizes CRC cells to thapsigargin-induced ER stress

We therefore investigated the functional role of TRAP1/TBP7 interaction. Several data suggests that ER stress, worsened by the high ROS concentrations in this sub-cellular compartment, is controlled by networks of molecular chaperones (21). Considering the previously described protective role of TRAP1 against several stresses, including oxidative stress through its antioxidant functions (4, 22), we hypothesized that TRAP1/TBP7 interaction constituted an additional control to check the

state/folding of proteins damaged in the ER. In order to induce protein misfolding in the ER, we induced ER stress by thapsigargin (TG), a well-known agent that mobilizes Ca^{2+} from the ER (23). As a marker of ER stress, we analyzed the expression of BiP/Grp78, a major ER chaperone protein essential for protein quality control in the ER, as well as a central regulator of the UPR (24). Figure 2 shows that BiP mRNA expression is strongly increased, upon TG treatment, in TRAP1-interfered cells, compared to the respective control (Panels A and B). Interestingly, a rescue of this phenotype is achieved upon TRAP1 re-addition (Panel B). These results demonstrate that TRAP1 knock down sensitizes cells to TG-induced ER stress, thus suggesting an involvement of this protein in ER stress response, as recently reported (10, 11).

We and other groups have previously demonstrated the protective roles of TRAP1 against cell death induced by several agents (4, 6). Therefore, we addressed whether TRAP1-interfered cells become more sensitive to apoptosis, as a possible and expected consequence of increased ER stress, and if TBP7 might play a role in this process. Table 1 shows that TRAP1 and TBP7 interference sensitized HCT116 cells to TG-induced apoptosis. Noteworthy, a similar result was observed upon cell treatment with oxaliplatin, a genotoxic agent (Table 1). Taken together, all these observations confirm the well-known role of TRAP1 in the protection against stress-induced cell death and highlight a new role for regulatory proteasome proteins in apoptotic control.

TRAP1/TBP7 control of intracellular protein ubiquitination

We then hypothesized that if the level of protein damage upon ER stress is too severe to be counteracted/repaired by TRAP1 refolding, increased protein degradation might occur, and increased ubiquitination levels of intracellular proteins could be observed. Indeed, tight regulation of protein ubiquitination by TRAP1/TBP7 does occur: in fact, a low Ubiquitin (Ub) signal is observed in TRAP1 containing cells, whereas TRAP1 interference strongly increases general protein ubiquitination levels (Figure 3).

The control of intracellular proteins ubiquitination by TRAP1/TBP7 is a general phenomenon since it is present in total extracts (Figure 3, Panel A). Interestingly, both TRAP1 and TBP7 seem to play a critical

role in the regulation of protein ubiquitination. In fact, upon the transfection of TRAP1 expression vectors in sh-TRAP1 stable transfectants a rescue of the high ubiquitin "phenotype" is observed (Figure 3, Panel A). A sub-cellular fractionation allowed us to demonstrate that this regulatory role is more evident in the post-mitochondrial fraction (cytosol+microsomes), where TRAP1/TBP7 control is particularly necessary given the abundance of proteins translated, but often damaged. Conversely, the same regulation is not observed in mitochondrial extracts even after retransfection of TRAP1, likely because TBP7 is absent in these organelles (Figure 3, Panel B). These results confirm that TRAP1 function in the regulation of protein ubiquitination requires the presence of TBP7. Additionally, increased cellular levels of ubiquitinated proteins, very similar to those obtained in cells transiently transfected with TRAP1 siRNAs, were observed upon TBP7 siRNA transfection (Figure 3, Panel C), thus confirming the role of TBP7 in this regulation. Altogether, these results demonstrated that TRAP1/TBP7 interaction is a useful and important check point in which these two proteins concomitantly work to judge whether a protein can be repaired and reach the final destination or, if the damage is too severe, it needs to be degraded. Furthermore, despite the block of proteasome activity by MG132 treatment, the experiments shown in Figure 3 demonstrate that the regulation of protein ubiquitination by TRAP1 is not due to inhibition of proteasome function, since it is observed also in the absence of the inhibitory drug (Figure 3, Panel A). Indeed, this finding was confirmed by assaying the proteasome's activity *in vitro* using fluorescent substrates and extracts from scramble and TRAP1- or TBP7-interfered cells. The results shown in Figure 3, Panel D demonstrate that neither TRAP1 nor TBP7 interference inhibit the proteasome's function.

More importantly we asked whether the control of protein ubiquitination by TRAP1/TBP7 requires TRAP1 mitochondrial localization. To address this issue we generated the Δ1-59 deletion mutant of TRAP1 (in which the first 59 aa containing the mitochondrial targeting sequences (MTS, 2) were removed from the N-terminus) yielding a TRAP1 mutant defective for mitochondrial import, but still able to bind TBP7 (Supplementary Figure 1 and Figure 4 Panels A-B). Interestingly, the transfection of this mutant in sh-TRAP1 stable clones rescued the heavy ubiquitin levels present in TRAP1-interfered cells (Figure 4 C). Conversely, another TRAP1 deletion mutant (Δ101-221) was generated that keeps the

MTS (Supplementary Figure 1) and, thus, is able to localize into mitochondria, but is unable to bind TBP7 which, as previously shown, is absent in the mitochondrial fraction. The transfection of the Δ101-221 mutant in sh-TRAP1 cells showed no changes in protein ubiquitination levels (Figure 4, Panels D-F). These experiments provide a proof of concept that the relevant amount of TRAP1 present in the ER fractions (see EM quali/quantitative analyses shown in Figure 1E) is indeed involved in the regulation of protein ubiquitination through its binding to TBP7, whereas mitochondrial TRAP1 does not influence ubiquitin levels, according to the phenotype generated by the Δ101-221 TRAP1 deletion mutant. Finally, we demonstrated that the transfection of TRAP1 Δ1-59 mutant decreased BiP/Grp78 mRNA levels present in sh-TRAP1 clones upon thapsigargin-induced ER stress. Figure 4, Panel G shows that a rescue of BiP/Grp78 mRNA levels is obtained upon the transfection of Δ1-59 mutant, whereas the Δ101-221 TRAP1 mutant with mitochondrial localization not only is unable to counteract ER stress, but even further increased BiP/Grp78 levels.

Strikingly, a TBP7 deletion mutant (Supplementary Figure 1), unable to bind TRAP1 (Figure 4, Panel H), yields, upon transfection in HCT116 cells (scramble), a strong ubiquitin pattern undistinguishible from the phenotype of sh-TRAP1 stable transfectants (Figure 4, Panel I), likely acting as dominant negative over the endogenous TBP7 protein's function.

Quality control of specific mitochondrial-destined proteins by TRAP1/TBP7

Once we demonstrated the contribution of TRAP1/TBP7 to the regulation of ER stress/apoptosis, with the consequent modulation of intracellular protein ubiquitination, we hypothesized that TRAP1 could be involved in a general control of protein stability. To this aim, pulse-chase experiments were performed in scramble and sh-TRAP1 stable transfectants. However, a comparable pattern of degraded proteins is still observed 72 h after Met/Cys chase (Figure 5, Panel A). This unchanged overall protein stability led us to hypothesize that TRAP1 could be involved in the control of protein folding/stability for selective proteins, likely those directed to mitochondria. To evaluate this hypothesis, the levels of F1ATPase, a nuclear-encoded mitochondrial protein and a potential TRAP1 interactor as suggested by MS analysis (12), were analyzed in cells in which TRAP1 expression was lowered by shRNA interference. Interestingly, protein levels decreased in TRAP1

stably interfered cells (Figure 5, Panel B and Supplementary Figure 2), whereas a rescue was obtained upon readdition of Δ1-59 TRAP1 mutant, but not by Δ101-221 TRAP1 mutant (Supplementary Figure 3). These findings confirm that the regulation of the observed phenomena occurs in the cytosolic compartment and support our model. Accordingly, the protein levels of p18 Sorcin, another mitochondrial protein, recently identified by our group as a novel mitochondrial Sorcin isoform interacting with TRAP1 (12), decreased upon TRAP1 interference (Figure 5, Panel B, arrow). Of note, in the same experimental conditions, no differences were observed in the protein levels of the higher mobility p22 Sorcin isoform, which shares high homology with the p18 Sorcin, but is not a mitochondrial protein, neither is a TRAP1 "partner" (Figure 5, Panel B, 12). Therefore, we hypothesize that the decreased expressions of F1ATPase and p18 Sorcin in mitochondria of TRAP1-interferred cells were dependent on increased ubiquitination. To this aim, the respective ubiquitination levels in scramble and TRAP1-inteferred cells were analyzed. Figure 5 (Panels C and D) shows that both proteins are more ubiquitinated in sh-TRAP1 transfectants. Accordingly, increased levels of ubiquitinated F1ATPase were induced upon TBP7 interference (Figure 5 , Panel E).

Finally, we evaluated whether TRAP1/TBP7 interaction and the relative effects on protein levels would have an impact *in vivo*. To this aim, we analyzed our tissue collection of CRCs, previously characterized for TRAP1 and Sorcin expression by immunoblot analysis (12). We observed that all CRCs overexpressing 18kDa Sorcin isoform (11/59 cases) shared the concomitant up-regulation of TRAP1. Therefore, we analyzed for TRAP1, Sorcin, F1ATPase and TBP7 expression the 11 Sorcin-ovexpressing tumors and, as controls, other 14 CRC specimens. Figure 6 reports the immunoblot analysis of the 4 proteins in 4 tumor samples representative of our tumor collection, whereas the expression profile of the 4 genes in 25 CRCs is reported in Supplementary Table 2. Remarkably, the majority of the p18 Sorcin- and TRAP1-positive tumors exhibited the up-regulation of TBP7 (9/11 cases) and F1ATPase (8/11 cases). By contrast, among 8 tumors with low expression of TRAP1, all exhibited low levels of TBP7 and p18 Sorcin and 7/8 low expression of F1ATPase. Chi-square test

demonstrated a positive statistical correlation between the expression levels of TRAP1 and those of Sorcin, F1ATPase and TBP7 (Supplementary Table 2).

DISCUSSION

TRAP1 was identified by our group as one of the proteins involved in and important for the homeostasis of osteosarcoma cells adapted to mild oxidative stress (4). The control of the protein folding environment in sub-cellular organelles, such as mitochondria, is important for adaptive homeostasis and may participate in human diseases, but the regulators of this process are still largely elusive. During the preparation of this manuscript, Altieri et al. (10) demonstrated that selective targeting of HSP90 chaperones in mitochondria of human tumor cells triggered compensatory autophagy, and an organelle UPR enhanced tumor cell apoptosis initiated by death receptor ligation, and inhibited tumor growth in mice without detectable toxicity. These results reveal a novel role of HSP90 chaperones in the regulation of the protein-folding environment in mitochondria of tumor cells.

Starting from the above observations and in agreement with Altieri's results, here we demonstrate an additional role of TRAP1 in protein quality control, acting on the outside of the ER. This TRAP1 function requires TBP7, a protein of the 19S proteasome regulatory subunit. As demonstrated by mass spectra analysis, this AAA-ATPase is a novel TRAP1-interacting protein whose role is determinant in the quality control of proteins. In fact, the interference of either TRAP1 or TBP7 proteins resulted both in the induction of apoptosis in response to both TG-induced ER stress or oxaliplatin treatment, and in increased intracellular protein ubiquitination, which was selectively rescued by the re-addition of TRAP1. Interestingly, TRAP1/TBP7 regulation of cellular ubiquitination is independent of modulation of proteasome function, since an *in vitro* assay of proteasome activity shows that TRAP1/TBP7 interference does not affect proteasome functionality. In contrast to current models of protein misfolding, where abnormal accumulation of ubiquitinated protein is prominent, cytosolic ubiquitin staining is dramatically reduced in Grp78 null Purkinje

cells (25). A plausible explanation is that BiP/Grp78, which unlike TRAP1 is a typical ER luminal chaperone (26), is required for ER protein retrotranslocation to be ubiquitinated in the cytosol. In this light, the presence of an additional chaperone just outside the ER might contribute to the control of protein folding as a compensatory mechanism in some abnormal biological processes. Furthermore, another chaperone and TRAP1 homolog, Grp94, is present in the ER, and its most important activity is to direct the folding and/or assembly of secreted and membrane proteins (27).

The regulatory networks that control the protein folding machinery in mitochondria are still largely elusive. In this regard, the demonstration that regulation of protein quality control by TRAP1 is directed toward mitochondrial proteins, expands the currently rather limited list of mitochondrial proteasome targets. It is reasonable to hypothesize that multiple chaperone networks control the misfolding of proteins addressed to different sub-cellular compartments. In this study, an additional "pre"-screening for proteins directed to mitochondria is characterized: if the protein is highly damaged and not successfully refolded by the chaperone machineries inside or outside the ER, including TRAP1, it will be identified by the regulatory proteosome protein, and targeted for degradation. TRAP1-containing supramolecular complexes might be present just outside the mitochondria, and in the cellular compartment of the tight ER-mitochondria interface (28 and Figure 1 Panel E), where proteasomes have also been identified (29) and ensure that among all the proteins translated in the ER, only undamaged proteins could enter into the mitochondria. Very recently, Takemoto *et al.* suggested that mitochondrial chaperone TRAP1 regulates the UPR in the ER, even though its presence in the ER has not been reported (11). Therefore, the demonstration that TRAP1 is present also on the external side of the ER is an important achievement strongly supporting its role in protection against stress.

The 26S proteasome is an enzymatic complex that degrades ubiquitinated proteins in eukaryotic cells. It is made up of the 20S CP and the 19S RP. The latter is further divided into the lid and base sub-complexes. While the mechanism involved in the assembly of the CP is well investigated, that of the RP is poorly understood. Some data report that proteasome base assembly is facilitated by

multiple proteasome-dedicated chaperones (14, 30). Even though we cannot exclude TRAP1 involvement in the regulation of proteasome assembly, our data suggest that proteasome activity is not affected by TRAP1 interference.

A still unsolved question is the mechanistic link between TRAP1-dependent mitochondrial adaptive response to stress and regulation of gene expression. Interestingly, some analyses have demonstrated the importance of 19S ATPases in the assembly of transcription machinery and provided additional insight into the regulatory mechanisms of the 19S proteasome in mammalian transcription (17). This hypothesis, although very attractive, requires further studies aimed to evaluate whether TBP7 could directly collaborate with TRAP1 in the regulation of gene expression. Alternatively, it could be hypothesized that mitochondrial chaperones may regulate gene expression by modulating ER stress. In support of this hypothesis, our results suggest that TRAP1 may be involved in the ER stress response. Furthermore, an interaction between TRAP1 and Sorcin, a calcium-binding protein, was characterized by our group (12), which might contribute to a regulatory role of TRAP1 and TRAP1-interacting proteins in ER stress induced by perturbation of calcium homeostasis (Maddalena et al, manuscript submitted) and protein quality control.

We did not observe any strong differences in mitochondrial protein ubiquitination upon modulation of TRAP1 levels. Quality control of mitochondrial proteins must be monitored by molecular chaperones (31). Only very small numbers of mitochondrial proteins are currently known to be degraded in a proteasome-dependent fashion (32), so a more focused effort to identify such additional substrates might dramatically expand the list of mitochondrial proteasome targets. Our results demonstrate that the expression of p18 Sorcin and F1-ATPase is decreased upon TRAP1 interference as a consequence of their increased ubiquitination. The identification of TRAP1/TBP7 specific “substrates” strongly contributes to the complex study of mitochondrial protein quality control. One reason for ubiquitination of mitochondrial proteins may be that when mitochondria-destined proteins are mistargeted or misfolded, they are identified as aberrant and recognized by the Ubiquitin Proteasome System (UPS) for removal. This may even support a role of the cytosolic UPS

in controlling levels and/or quality of proteins destined for mitochondria. In addition, the presence of TRAP1 on the outer side of ER and the absence of TBP7 in mitochondria suggest that TRAP1 functions in these latter organelles are not directly linked to ubiquitination control, whereas this control is present in a different compartment and requires interaction with TBP7. In support of this model are the results of transfection experiments with newly generated TRAP1 mutants, either able to interact with TBP7 and localized in the ER/cytosol fractions (Δ1−59) or unable to bind TBP7, but imported into mitochondria (Δ101-221). Indeed, only the mitochondrial import-defective Δ1−59 mutant, and not the mitochondrial Δ101-221 deletion mutant, rescues the strong ubiquitin levels in sh-TRAP1 interfered cells. These findings provide a proof of concept that protein quality control depends on the cytosolic interaction between TRAP1 and TBP7. Consistent with these results is the observation that again only the Δ1−59 TRAP1 mutant rescues the decreased levels of TRAP1-regulated proteins (Supplementary Figure 3), as well as the levels of BiP/Grp78 mRNA upon thapsigargin-induced ER stress (Figure 4, Panel G). All these observations are in agreement with still unidentified proteasome members in mitochondria, even though several proteases, ATPases and ubiquitin ligases have been identified (33). Furthermore, a functional interplay between mitochondrial and proteasome activity has been demonstrated, thus suggesting that both systems are interdependent (34).

Remarkably, the finding that the proposed TRAP1 network is conserved in CRCs is consistent with our model and provides new insights into the quality control/stability/ubiquitination of proteins in human cancer, a still highly debated issue. Indeed, the proteotoxic stress generated by accumulation of misfolded proteins and the consequent heat shock response is currently under evaluation as a potential anticancer treatment target, since many tumor cells display constitutive proteotoxic stress and dependence on heat shock response due to their rapid rates of proliferation and translation (35). The induction of proteotoxic stress via stimulation of protein misfolding (hyperthermia, radiofrequency ablation), inhibition of proteasomes (by bortezomib) or inhibition of HSP90 (by geldanamycin) have all been evaluated or used for cancer treatment. Interestingly, bortezomib, a

reversible inhibitor of the 26S proteasome, is at present a valuable option for the first-line treatment of multiple myeloma (36). Thus, the characterization of TRAP1, a chaperone up-regulated in about 60% of human CRCs (5), as a protein involved in quality control and in protection against apoptosis in cancer cells provides a strong rationale for considering this network as a novel molecular target for the treatment of human CRC.

In summary, a new crosstalk between ER and mitochondria is suggested and summarized in the working model, as shown in Figure 7. Our study demonstrates for the first time that TRAP1 is also present in the ER of cancer cells where it is involved in the quality control and intracellular protein ubiquitination of mitochondria-destined proteins, through a direct interaction (as demonstrated by the FRET analysis shown in Figure 1, Panel D) with TBP7, one of the proteins present in the regulatory proteasome subunit. Thus, a "customs office" could be hypothesized at the ER/mitochondria interface, with TRAP1 and TBP7 being the officers at this important check point. These two officers, each with independent but related functions, help to judge whether a protein can be repaired and reach its final mitochondrial destination or, if the damage is too severe, it needs to be degraded.

Materials and methods

Cell culture, plasmids generation and transfection procedures

HCT116 cells were cultured in DMEM supplemented with 10% fetal bovine serum (FBS) in standard conditions. Full-length TRAP1 and Sorcin expression vectors were obtanined as previously described (12).

Mutant Δ1-59-Myc was generated with the following primers: Δ1-59-myc, forward 5'-*ATTAGAATTCATGAGCACGCAGACCGCCGAGG*-3'; reverse 3'-*ATTACTCGAGGTGTCGCTCCAGGGCCTTGA*-5'. PCR-amplified fragments were gel-purified and cloned in frame into pcDNA 3.1 plasmid (Invitrogen, San Giuliano Milanese, Italy) at the Eco-RI and XhoI restriction sites.

Mutant Δ101-221- HA was generated using the following primers: TRAP1-HA, forward 5'-atta *GCGGCCGCGCAGCCAACATGGCGCGCGAGCCTGCGGG*-3'; reverse 5'atta*TCTAGATTAAGCGTAATCTGGAACATCATATGGGTATCAGTGTCGCTCCAGGGCCTTGA*-3'; Δ101-221-HA, forward 5'-atta*CCGCGGTCGGCAGCCCCGGGGAGCCT*-3'; reverse 5'-atta*CCGCGGAAACACCTCTTTTTCTGAGT*-3'. The PCR products obtained with the primers TRAP1-HA forward and Δ101-221-HA reverse were cloned in pRc-CMV vector (Invitrogen, San Giuliano Milanese, Italy); the PCR product obtained with the primers ΔATPase-HA forward and TRAP1-HA reverse was subcloned in the same plasmid. All clones were sequenced to confirm identity and PCR fidelity.The plasmid pCMV5L/S6 (TBP7-HA) was a kind gift of Dr. Simon Dawson, University of Nottingham.

Mutant ΔTBP7-FLAG was generated by excising a fragment from the full-length TBP7 expression vector using EcoRI and BamHI restriction endonucleases. The fragment was gel-purified and cloned into the corresponding sites of the expression vector p3x-FLAG.

Transient transfection of DNA plasmids was performed with Polyfect Transfection reagent (Qiagen, Milan, Italy). siRNAs of TRAP1 and TBP7 were purchased from Qiagen, Milan, Italy (Cat. No. S100301469 for TBP7, SI00115150 for TRAP1). For knockdown experiments, siRNAs were diluted to a final concentration of 20 nmol/L and transfected according to the manufacturer's protocol. For control experiments, cells were transfected with a similar amount of scrambled RNA (Qiagen, Milan, Italy, Cat. No. SI03650318). Transient transfections of siRNAs were performed by using HiPerFect Transfection Reagent (Qiagen, Milan, Italy). TRAP1-stable interference was achieved by transfecting HCT116 cells with TRAP1 (TGCTGTTGACAGTGAGCGACCCGGTCCCTGTACTCAGAAATAGTGAAGCCACAGATGT ATTTCTGAGTACAGGGACCGGGCTGCCTACTGCCTCGGA) or scrambled (sequence containing no homology to known mammalian genes) short hairpin RNAs (shRNA) (Open Biosystems, Huntsville, AL, USA).

Cell extracts, purification and treatments

Total cell lysates were obtained by homogenization of cell pellets and tumor specimens in cold lysis buffer (20mM Tris, pH 7.5 containing 300mM sucrose, 60mM KC1, 15mM NaC1, 5% (v/v) glycerol, 2mM EDTA, 1% (v/v) Triton X-100, 1mM PMSF, 2 mg/ml aprotinin, 2 mg/ml leupeptin and 0.2% (w/v) deoxycholate) for 1 min at 4°C and further sonication for 30 sec at 4°C. For ER stress induction, cells were treated overnight with 1μM thapsigargin (Sigma-Aldrich, Milan, Italy) before harvesting.

Mitochondria and ER were purified using the Qproteome Mitochondria Isolation Kit (Qiagen, Milan, Italy) according to the manufacturer's protocol and as elsewhere described (12). Briefly, HCT116 cells were washed and suspended in lysis buffer, which selectively disrupts the plasma membrane without solubilizing it, resulting in the isolation of cytosolic proteins. Plasma membranes and compartmentalized organelles, such as nuclei, mitochondria, and ER, remained intact and were pelleted by centrifugation. The resulting pellet was resuspended in disruption buffer, repeatedly passed through a narrow-gauge needle (to ensure complete cell disruption), and centrifuged to pellet nuclei, cell debris, and unbroken cells. The supernatant (containing mitochondria and the microsomal fraction) was recentrifuged to pellet mitochondria. The resulting supernatant (microsomal fraction) was treated with proteinase K for 20 min on ice ± NP40 (Igepal, Sigma-Aldrich, Milan, Italy) according to Hassink et al. (37). or with 0.1 M Na2CO3 pH 11.3 for 30 min to remove peripheral ER membrane proteins (38)

Western blot analysis and antibodies

Equal amounts of protein from cell lysates and tumor specimens were subjected to 10% (v/v) SDS-PAGE and transferred to a PVDF membrane (Millipore, Temecula, CA, USA). The membrane was blocked with 5% (w/v) skim milk and incubated with primary antibody, followed by incubation with an HRP-conjugated secondary antibody. Proteins were visualized with an ECL detection system (GE Healthcare, Waukesha, Wisconsin, USA). The following antibodies from Santa Cruz Biotechnology, Segrate, Italy were used for WB analysis and immunoprecipitation: anti-TRAP1 (sc-13557), anti-Sorcin (sc-100859), anti-TBP7 (sc-166003), anti-cMyc (sc-40), CypD (sc-82570),

VDAC (sc-8830), HSP60 (sc-1052), anti-ubiquitin (sc-8017), anti-COX4 (sc-58348), anti-F1ATPase (ATP5B subunit, sc-58619), anti-tubulin (sc-8035), anti-HA (sc-805), and anti–glyceraldehyde-3-phosphate dehydrogenase (GAPDH; sc-69778). Rabbit polyclonal anti-calnexin antibody (BD Biosciences, Milan, Italy), were also used.

RNA extraction and semiquantitative and Real Time RT-PCR analysis.

Total RNA from cell pellets and tumor specimens was extracted using the TRIzol Reagent (Invitrogen, San Giuliano Milanese, Italy). For the first strand synthesis of cDNA, 3μg of RNA were used in a 20 μl reaction mixture utilizing a cDNA Superscript II (Invitrogen, San Giuliano Milanese, Italy). For Real Time PCR analysis, 1 μl of cDNA sample was amplified using the Platinum SYBR Green qPCR Supermix UDG (Invitrogen, San Giuliano Milanese, Italy) in an iCycler iQ Real Time Detection System (BioRad Laboratories GmbH, Segrate, Italy). The following primers were utilized: BiP/Grp78, forward 5'-*CGTGGATGACCCGTCTGTG*-3', reverse 5'-*CTGCCGTAGGCTCGTTGATG*-3' (PCR product 308 bp); GAPDH, forward 5'-*CAAGGCTGAGAACGGGAA*-3', reverse 5'-*GCATCGCCCCACTTGATTTT*-3' (PCR product 90 bp). Primers were designed to be intron spanning. Reaction conditions were 50° C for 2 min, 95°C for 2 min, followed by 45 cycles of 15 s at 95°C, 30 s at 60°C, 30 s at 72°C. GAPDH was chosen as an internal control.

For semiquantitative RT-PCR, RNA obtained by scramble and sh-TRAP1 HCT116 cells was retro-transcribed and amplified with specific primers for Bip/Grp78 and GAPDH using the Superscript III-One STEP Kit (Invitrogen, San Giuliano Milanese, Italy), according to the manufacturer's instructions. The following primers were used to amplify the corresponding transcripts: GAPDH, forward 5′-*GAA GGT GAA GGT CGG AGT C*-3′, reverse 5′-*GAA GAT GGT GAT GGG ATT TC*-3′, BiP/Grp78, forward 5'-*CTG GGT ACA TTT GAT CTG ACT GG*-3', reverse 5'-*GCA TCC TGG TGG CTT TCC AGC CAT TC*-3'. The primers of BiP/Grp78 were a kind gift from Prof. P. Remondelli, University of Salerno, Italy.

Apoptosis assay

HCT116 cells were subjected to downregulation of TRAP1 and TBP7 expression by siRNA transfection. Apoptosis was evaluated by cytofluorimetric analysis of annexin V and 7-amino-actinomycin D (7-AAD) positive cells using the FITC-Annexin V/7-AAD Kit (Beckman Coulter, Cassina De' Pecchi – Milan, Italy). Stained cells were analyzed by the "EPICS XL" Flow Cytometer (Beckman Coulter, Cassina De' Pecchi – Milan, Italy). Ten thousand events were collected per sample. Positive staining for annexin V, as well as double staining for annexin V and 7-AAD were interpreted as signs of, respectively, early and late phases of apoptosis (39). Experiments were performed three times using three replicates for each experimental condition.

Immunofluorescence, confocal-microcopy and EM analysis

HCT116 cells were fixed with 0.1M phosphate buffer containing 4% (w/v) paraformaldehyde for 15 minutes, then blocked and permeabilized with 5% (w/v) BSA, 0.1% (v/v) Triton X-100, 10% (v/v) FBS in PBS for 20 min at RT before staining with primary antibodies (for TRAP1, CALNEXIN and TBP7) and corresponding secondary TEXAS RED/FITC-conjugated antibodies. The analysis of immunofluorescence was performed with a confocal laser scanner microscopy Zeiss 510 LSM (Carl Zeiss Microimaging, Göttingen, Germany), equipped with Argon ionic laser (Carl Zeiss Microimaging, Göttingen, Germany) whose λ was set up to 488 nm, a HeNe laser whose λ was set up to 546 nm, and an immersion oil objective, 63 ×/1.4 f. For the immuno-EM analysis, cells were fixed with a mixture of 4% (v/v) paraformaldehyde and 0.05% (v/v) glutaraldehyde, labeled with a monoclonal antibody against HA using the gold-enhance protocol, embedded in Epon-812, and cut as described previously (40). EM images were acquired from thin sections using an FEI Tecnai-12 electron microscope equipped with an ULTRA VIEW CCD digital camera (FEI, Eindhoven, The Netherlands). Thin sections were also used for quantification of gold particles residing within mitochondria using the AnalySIS software (Soft Imaging Systems GmbH, Munster, Germany).

FRET experiments

FRET was measured by using the acceptor photo-bleaching technique (20) where, upon irreversible photo-bleaching, the donor fluorescence increase was recorded. Cells on coverslips were fixed,

immuno-stained with specific anti-TBP7 and anti-TRAP1 antibodies and secondary antibodies conjugated respectively with Cy3 and Cy5 and mounted in PBS/Glycerol (1:1). Images were collected using a laser scanning confocal microscope (Zeiss LSM 510 Meta) equipped with a planapo 63x oil-immersion (NA 1.4) objective lens. Laser lines at 543 nm and 633 were used to excite respectively the fluorophores Cy3 and Cy5. For Cy5 bleaching, the 633 nm HeNe laser light with 100% of output power was used and pinhole diameters were set to have 1.0 um optical slices.

FRET measurements were performed using the LSM software (LSM Zeiss, Germany) after photo-bleaching of a selected square ROI of 6 μm^2. We calculated the FRET efficiency on the basis of the following equation: E = (fluorescence intensity Cy3 post-bleaching - fluorescence intensity Cy3 pre-bleaching)/ fluorescence intensity Cy3 post-bleaching (20)**.**

As control we measured FRET on cells expressing TBP7 alone labelled with Cy3 in order to ensure that photo-bleaching *per se* does not affect the fluorescence of the donor and that photo-conversion does not occur during the photo-bleaching analysis. We calculated the background raised by the photobleaching *per se* by bleaching Cy5 in cells negative for this fluorophore. The background value was subtracted from all samples.

Pulse-chase assay

Pulse-chase analysis was performed as described elsewhere (41). In brief, HCT116 cells were incubated in cysteine/methionine-free medium (Sigma-Aldrich, Milan, Italy) for 1 h followed by incubation in cysteine/methionine-free medium containing 50 μCi/mL ^{35}S-labeled cysteine/methionine (GE-Healthcare, Waukesha, Wisconsin, USA) for 1 h. After labelling, cells were washed once with culture medium containing 10-fold excess of unlabeled methionine and cysteine (5mM each) and incubated further in the same medium for the indicated times. Cells were collected at the indicated time points, and separated on 10% SDS–PAGE. Proteins were transferred onto a PVDF membrane (Millipore, Temecula, CA, USA) and probed by WB analysis.

Patients

Between May 2008 and May 2011, specimens from both tumor and normal, non-infiltrated peritumoral mucosa were obtained from 59 patients with CRC during surgical removal of the neoplasm. Samples were divided into 125 mm^3 pieces, one specimen was fixed in formalin and used for the histopathological diagnosis, while the others were immediately frozen in liquid nitrogen and stored at –80°C for immunoblot analysis. Samples were analyzed within 30 days after collection and were thawed only once. Express written informed consent to use biological specimens for investigational procedures was obtained from all patients.

Statistical Analysis.

Chi-square test was used to establish the statistical correlation between the expression levels of TRAP1 and those of Sorcin, F1ATPase and TBP7 in human colorectal carcinomas. Statistically significant values ($p<0.05$) are reported in the Results.

Acknowledgments

This work was supported by Grants IG8780 from the Associazione Italiana per la Ricerca sul Cancro (AIRC), Ministero dell'Istruzione dell'Università e della Ricerca (PRIN 2008), Fondazione Berlucchi to M.L. and F.E. Our special thanks to Anthony Green for proofreading the manuscript and suggesting stylistic improvements, as well as to the Mass Spectrometry Unit (CEINGE Biotecnologie Avanzate, Naples, Italy), Telethon Electron Microscopy Core Facility (TeEMCoF, IBP, CNR, Naples) and Integrated Microscopy Facility (IGB, CNR, Naples) for EM assistance.

References

1. Song HY, Dunbar JD, Zhang YX, Guo D and Donner DB Identification of a protein with homology to HSP90 that binds the type 1 tumor necrosis factor receptor. J. Biol. Chem. 1995; 270: 3574-3581

2. Felts SJ, Owen BA, Nguyen P, Trepel J, Donner DB and Toft DO The HSP90-related protein TRAP1 is a mitochondrial protein with distinct functional properties. J. Biol. Chem. 2000; 275(5): 3305–3312
3. Montesano Gesualdi N, Chirico G, Catanese MT, Pirozzi G and Esposito F AROS-29 is involved in adaptive response to oxidative stress. Free Radic. Res. 2006; 40(5): 467-476
4. Montesano Gesualdi N, Chirico G, Pirozzi G, Costantino E, Landriscina M and Esposito F Tumor necrosis factor-associated protein 1 (TRAP-1) protects cells from oxidative stress and apoptosis. Stress 2007; 10(4): 342-350
5. Costantino E, Maddalena F, Calise S, Piscazzi A, Tirino V, Fersini A, et al TRAP1, a novel mitochondrial chaperone responsible for multi-drug resistance and protection from apoptosis in human colorectal carcinoma cells. Cancer Lett. 2009; 279(1): 39-46
6. Kang BH, Plescia J, Dohi T, Rosa J, Doxsey SJ and Altieri DC Regulation of tumor cell mitochondrial homeostasis by an organelle-specific HSP90 chaperone network. Cell 2007; 131(2): 257-270
7. Leav I, Plescia J, Goel HL, Li J, Jiang Z, Cohen RJ, et al Cytoprotective mitochondrial chaperone TRAP-1 as a novel molecular target in localized and metastatic prostate cancer. Am. J. Pathol. 2010; 176(1): 393-401
8. Kang BH, Siegelin MD, Plescia J, Raskett CM, Garlick DS, Dohi T, et al Preclinical characterization of mitochondria-targeted small molecule HSP90 inhibitors, gamitrinibs, in advanced prostate cancer. Clin. Cancer Res. 2010; 16(19): 4779-4788
9. Kang BH, Tavecchio M, Goel HL, Hsieh CC, Garlick DS, Raskett CM, et al Targeted inhibition of mitochondrial HSP90 suppresses localised and metastatic prostate cancer growth in a genetic mouse model of disease. Br. J. Cancer 2011; 104(4): 629-634
10. Siegelin MD, Dohi T, Raskett CM, Orlowski GM, Powers CM, Gilbert CA, et al Exploiting the mitochondrial unfolded protein response for cancer therapy in mice and human cells. J. Clin. Invest. 2011; Mar 1 [Epub ahead of print]

11. Takemoto K, Miyata S, Takamura H, Katayama T and Tohyama M Mitochondrial TRAP1 regulates the unfolded protein response in the endoplasmic reticulum. Neurochem. Int. 2011; Feb 18. [Epub ahead of print]
12. Landriscina M, Laudiero G, Maddalena F, Amoroso MR, Piscazzi A, Cozzolino F, et al Mitochondrial chaperone TRAP1 and the calcium binding protein Sorcin interact and protect cells against apoptosis induced by antiblastic agents. Cancer Res. 2010; 70(16): 6577-6586
13. Marx FP, Soehn AS, Berg D, Melle C, Schiesling C, Lang M, et al The proteasomal subunit S6 ATPase is a novel synphilin-1 interacting protein--implications for Parkinson's disease. FASEB J. 2007; 21(8): 1759-1767
14. Kaneko T, Hamazaki J, Iemura S, Sasaki K, Furuyama K, Natsume T, et al Assembly pathway of the Mammalian proteasome base subcomplex is mediated by multiple specific chaperones. Cell 2009; 137(5): 914-925
15. Landriscina M, Amoroso MR, Piscazzi A and Esposito F Heat shock proteins, cell survival and drug resistance: the mitochondrial chaperone TRAP1, a potential novel target for ovarian cancer therapy. Gynecol. Oncol. 2010; 117(2): 177-182
16. Landriscina M, Maddalena F, Laudiero G and Esposito F Adaptation to oxidative stress, chemoresistance, and cell survival. Antioxid. Redox Signal. 2009; 11(11): 2701-2716
17. Truax AD, Koues OI, Mentel MK and Greer SF The 19S ATPase S6a (S6'/TBP1) regulates the transcription initiation of class II transactivator. J. Mol. Biol. 2010; 395(2): 254-269
18. Tsai YC and Weissman AM The Unfolded Protein Response, degradation from endoplasmic reticulum and cancer. Genes Cancer 2010; 1(7): 764-778
19. Ohana B, Moore PA, Ruben SM, Southgate CD, Green MR and Rosen CA The type 1 human immunodeficiency virus Tat binding protein is a transcriptional activator belonging to an additional family of evolutionarily conserved genes. Proc. Natl. Acad. Sci. U.S.A. 1993; 90(1): 138-142

20. Kenworthy AK and Edidin M Imaging fluorescence resonance energy transfer as probe of membrane organization and molecular associations of GPI-anchored proteins. Methods Mol. Biol. 1999; 116: 37-49
21. Enyedi B, Várnai P and Geiszt M Redox state of the endoplasmic reticulum is controlled by Ero1L-alpha and intraluminal calcium. Antioxid. Redox Signal. 2010; 13(6): 721-729
22. Masuda Y, Shima G, Aiuchi T, Horie M, Hori K, Nakajo S, et al Involvement of tumor necrosis factor receptor-associated protein 1 (TRAP1) in apoptosis induced by beta-hydroxyisovalerylshikonin. J. Biol. Chem. 2004; 279(41): 42503–42515
23. Morales AP, Carvalho AC, Monteforte PT, Hirata H, Han SW, Hsu YT, et al Endoplasmic reticulum calcium release engages Bax translocation in cortical astrocytes. Neurochem. Res. 2011; Feb 24. [Epub ahead of print]
24. Chen WT and Lee AS Measurement and modification of the expression level of the chaperone protein and signaling regulator GRP78/BiP in mammalian cells. Methods Enzymol. 2011; 490: 217-233
25. Wang M, Ye R, Barron E, Baumeister P, Mao C, Luo S, et al Essential role of the unfolded protein response regulator GRP78/BiP in protection from neuronal apoptosis. Cell Death Differ. 2010; 17(3): 488-498
26. Zhang Y, Liu R, Ni M, Gill P and Lee AS Cell surface relocalization of the endoplasmic reticulum chaperone and unfolded protein response regulator GRP78/BiP. J. Biol. Chem. 2010; 285(20): 15065-15075
27. Eletto D, Dersh D and Argon Y GRP94 in ER quality control and stress responses. Semin. Cell Dev. Biol. 2010; 21(5): 479-485
28. Hayashi T and Su TP Sigma-1 receptor chaperones at the ER-mitochondrion interface regulate Ca(2+) signaling and cell survival. Cell 2007; 131(3): 596–610
29. Azzu V and Brand MD Degradation of an intramitochondrial protein by the cytosolic proteasome. J. Cell Sci. 2010; 123(Pt 4): 578-585

30. Roelofs J, Park S, Haas W, Tian G, McAllister FE, Huo Y, et al Chaperone-mediated pathway of proteasome regulatory particle assembly. Nature 2009; 459(7248): 861-865
31. Baker BM and Haynes CM Mitochondrial protein quality control during biogenesis and aging. Trends Biochem. Sci. 2011; Feb 24. [Epub ahead of print]
32. Livnat-Levanon N and Glickman MH Ubiquitin-proteasome system and mitochondria - reciprocity. Biochim. Biophys. Acta 2011; 1809(2): 80-87
33. Germain D Ubiquitin-dependent and -independent mitochondrial protein quality controls: implications in ageing and neurodegenerative diseases. Mol Microbiol. 2008; 70(6): 1334-1341
34. Kozieł R, Greussing R, Maier AB, Declercq L and Jansen-Dürr P Functional interplay between mitochondrial and proteasome activity in skin aging. J. Invest. Dermatol. 2011; 131(3): 594-603
35. Neznanov N, Komarov AP, Neznanova L, Stanhope-Baker P and Gudkov A Proteotoxic stress targeted therapy (PSTT): induction of protein misfolding enhances the antitumor effect of the proteasome inhibitor bortezomib. Oncotarget 2011; Mar 27. [Epub ahead of print]
36. Ludwig H, Beksac M, Bladé J, Cavenagh J, Cavo M, Delforge M, et al Multiple Myeloma Treatment Strategies with Novel Agents in 2011: A European Perspective. Oncologist 2011 Mar 26. [Epub ahead of print]
37. Hassink GC, Zhao B, Sompallae R, Altum M, Gastaldello S, Zinin NV, et al The ER-resident ubiquitin-specific protease19 participates in the UPR and rescues ERAD substrates. EMBO Rep. 2009; 10(7): 755-761
38. Fujiki Y, Hubbard AL, Fowler S and Lazarow PB Isolation of intracellular membranes by means of sodium carbonate treatment: application to endoplasmic reticulum. J. Cell Biol. 1982; 93: 97-102

39. George TC, Basiji DA, Hall BE, Lynch DH, Ortyn WE, Perry DJ, et al Distinguishing modes of cell death using the ImageStream multispectral imaging flow cytometer. Cytometry A 2004; 59: 237–245
40. Polishchuk EV, Di Pentima A, Luini A and Polishchuk RS Mechanism of constitutive export from the Golgi: bulk flow via the formation, protrusion, and en bloc cleavage of large trans-Golgi network tubular domains. Mol. Biol. Cell 2003; 14(11): 4470-4485
41. Lieberman AP, Harmison G, Strand AD, Olson JM and Fischbeck KH Altered transcriptional regulation in cells expressing the expanded polyglutamine androgen receptor. Hum. Mol. Genet. 2002; 11: 1967–1976

Titles and Legends to Figures

Figure 1: **TRAP1 and TBP7 interact and colocalize in the endoplasmic reticulum (ER)**

A) Total HCT116 lysates were harvested and immunoprecipitated with anti-TRAP1 and anti-TBP7 antibodies as described in Materials and Methods, separated by SDS-PAGE and immunoblotted with the indicated mouse-monoclonal anti-TRAP1 and mouse-monoclonal anti-TBP7 antibodies. No Ab, total cellular extracts incubated with A/G plus agarose beads without antibody; IP, immunoprecipitation with the corresponding antibodies.

B) Total HCT116 lysates were fractionated into mitochondrial (MITO), cytosolic (CYTO) and microsomal (ER) fractions as described in Materials and Methods, separated by SDS-PAGE and immunoblotted with mouse monoclonal anti-TRAP1 and mouse monoclonal anti-TBP7 antibodies. The purity of the fractions was assessed by using mouse monoclonal anti-tubulin, goat polyclonal anti-CypD, rabbit polyclonal anti-Calnexin antibodies specific for the single subcellular compartments.

C) TRAP1 and TBP7 co-immunoprecipitation analysis on the microsomal fraction (ER), obtained as described in Materials and Methods. Western blot of immunoprecipitates was performed with the indicated antibodies.

D) TRAP1/TBP7 direct interaction

FRET was measured by using the acceptor photo-bleaching technique as described in Materials and Methods. The pictures show the signal of TBP7 (red) and TRAP1 (green), before (a, b, c) and after photo-bleaching (d, e, f). The selected ROI for bleaching was indicated. Energy transfer efficiency was measured in cells transiently co-transfected with TRAP1 and either TBP7 or its mutant form (ΔTBP7-Flag) and was expressed in % as mean of 3 independent experiments. Error bars, ± SD. *p<0,0001.

E) ER Distribution of TRAP in HCT116 cells (EM microscopy)

Cells expressing TRAP-HA vector were fixed and prepared for immuno-EM (see Materials and Methods). Labeling with anti-HA antibody revealed significant amount of TRAP1 in mitochondria (a, b arrowheads). In addition, TRAP1 was distributed throughout the elongated membrane profiles (a, arrows) that on the basis of their ultrastructural features (such as attached ribosomes) can be attributed to the rough ER compartment, and detected along the nuclear envelope (b, arrows). The density of immuno-gold labeling (in arbitrary units; average±SD) in mitochondria (MITO), endoplasmic reticulum (ER) and endosomes (as a negative control) is reported in the lower histogram.

F) ER TRAP1/TBP7 colocalization (confocal microscopy)

Immunofluorescence shows TBP7 co-localization with TRAP1 and with the ER protein calnexin. In Panel 1, a double immunofluorescent staining is shown for TRAP1 (green) and TBP7 (red). In Panel 2, a double immunofluorescent staining is shown for calnexin (green) and TBP7 (red). In cells expressing the Myc-tagged TRAP1 construct (red) the protein co-distributes to a large extent with endogenous calnexin (green, Panel 3).

G and H) Biochemical characterization of TRAP1/TBP7 "topology" in the ER .

Western blot of HCT116 microsomal fractions treated with 0.4 μg/ml or 4 μg/ml proteinase K (pt K) ± 1% NP40 for 20 min on ice (Panel G) or with 100 mM Na_2CO_3 (pH 11.3) for 30 min (Panel H)

as described in Materials and Methods. Specific proteins were revealed with the indicated antibodies. Panel G**:** S, supernatant; P, pellet.

Figure 2: BiP mRNA levels in sh-TRAP1 stable clones.

A) Semiquantitative RT-PCR analysis of BiP/Grp78 mRNA expression in sh-TRAP1 stable clones respect to scrambled transfectants after 12 h treatment with 1μM thapsigargin (TG). As control, the levels of GAPDH transcript were analyzed.

B) Real Time RT-PCR analysis of BiP/Grp78 mRNA expression in scrambled and sh-TRAP1 HCT116 cells exposed to 1μM TG for 12 and in sh-TRAP1 HCT116 cells transfected with TRAP1 cDNA before treatment with TG. P values indicate the statistical significance between different Bip/Grp78 levels in the indicated conditions.

Figure 3: Ubiquitin levels in HCT116 cells.

A) Total cell lysates from sh-TRAP1 and scrambled HCT116 stable clones were transfected with either a HA-tagged ubiquitin vector (Ub-HA) or with TRAP1 expression vectors, treated with 1μM MG132 for 24 h, harvested 48 h after transfection and subjected to immunoblot with rabbit polyclonal anti-HA antibodies. The same filter was re-probed with mouse monoclonal anti-GAPDH antibodies for the normalization of cell lysates. Three independent experiments were performed with similar results.

B) Subfractionation of total lysates were obtained from sh-TRAP1 and scrambled HCT116 stable transfectants treated as described in A. The extracts from post-mitochondrial fraction (microsomes+cytosolic fraction) and mitochondria (MITO, see Materials and Methods) were separated by SDS-PAGE and immunoblotted with rabbit polyclonal anti-HA antibody to detect ubiquitin levels. The purity of fractions was verified with mouse-monoclonal anti-COX IV, or mouse monoclonal anti-GAPDH antibodies. Three independent experiments were performed with similar results.

C) HCT116 cells were co-transfected with an Ub-HA vector and siRNA negative control (scramble), or with siRNAs specific for TRAP1, TBP7, or both (as indicated) and total cell lysates harvested after 48 h from transfection. Total lysates were subjected to SDS-PAGE and immunoblotted with rabbit polyclonal anti-HA antibodies to detect total ubiquitin levels. The same filter was re-probed with mouse monoclonal anti-GAPDH antibodies for the normalization of cell lysates, and with mouse monoclonal anti-TRAP1, and mouse monoclonal anti-TBP7 antibodies.

D) Proteasome activity is not affected by TRAP1 and TBP7 silencing.

Total cellular extracts were prepared after 48 h transfection with specific siRNA for TRAP1, TBP7 or Sorcin, as control, or with siRNA negative control (scramble) and incubated in the presence of assay buffer and the fluorogenic substrate Suc-LLVY-AMC, as described in Materials and Methods. Samples were analyzed in triplicate using an excitation wavelength of 360 nm and an emission wavelength of 450 nm to detect chymotryptic proteasome activity. Data represent the mean of three independent experiments.

Figure 4: TRAP1/TBP7 interaction in ER is required for the control of protein ubiquitination and ER stress.

A and D) Subcellular localization of Δ1-59-Myc/Δ101-221-HA mutants

HCT116 cells were transfected with Δ1-59-Myc (Panel A) or Δ101-221-HA (Panel D) TRAP1 mutants, subfractionated into mitochondrial (MITO), cytosolic (CYTO) and microsomal (ER) fractions (Panel A) or mitochondrial (MITO) and post-mitochondrial (PM, cytosol+microsomes) fractions (Panel D), as described in Materials and Methods, separated by SDS-PAGE and immunoblotted with the indicated antibodies to verify the expression of mutants and the purity of fractions. For the details of mutant's generation procedures see Materials and Methods.

B and E) Interaction between Δ1-59-Myc/Δ101-221-HA mutants and TBP7

HCT116 cells were transfected with Δ1-59-Myc (Panel B) or Δ101-221-HA (Panel E) TRAP1 mutants, harvested and immunoprecipitated with anti-Myc or anti-HA antibodies as described in

Materials and Methods. Immunoprecipitates were separated by SDS-PAGE and immunoblotted with the indicated antibodies. No Ab, total cellular extracts incubated with A/G plus agarose beads without antibody; IP, immunoprecipitation with the corresponding antibodies. Three independent experiments were performed with similar results.

C) Ubiquitination levels upon transfection of Δ1-59-Myc TRAP1 deletion mutant

Total lysates from HCT116 scrambled, sh-TRAP1 stable clones and sh-TRAP1 cells transfected with Δ1-59-Myc TRAP1 mutant were subjected to immunoblot analysis with mouse monoclonal anti-Ubiquitin antibodies to detect total ubiquitination levels and with anti-GAPDH antibody for the normalization of cell lysates. Three independent experiments were performed with similar results.

F) Ubiquitination levels upon transfection of Δ101-221-HA TRAP1 deletion mutant

HCT116 scramble, sh-TRAP1 and sh-TRAP1 cells transfected with Δ101-221-HA TRAP1 mutant were subfractionated in post-mitochondrial (microsomes+cytosolic fraction) and mitochondrial (MITO) fractions as described in Materials and Methods. Total lysates from the same cells were used as controls (left panel). Protein lysates were subjected to immunoblot analysis with mouse monoclonal anti-Ubiquitin antibodies to detect total ubiquitination levels. The purity of fractions was verified with mouse monoclonal anti-GAPDH (left and right panels), and mouse-monoclonal anti-COX IV (middle panel) antibodies. Three independent experiments were performed with similar results.

G) Real Time RT-PCR analysis of BiP/Grp78 mRNA expression in scrambled and sh-TRAP1 HCT116 cells exposed to 1μM TG for 12 h (same as in Figure 2B) and in sh-TRAP1 HCT116 cells transfected with Δ1-59-Myc or Δ101-221-HA TRAP1 mutants, as indicated, before treatment with TG. P values indicate the statistical significance between different Bip/Grp78 levels in the indicated conditions.

H) Interaction between TRAP1 and ΔTBP7-Flag deletion mutant

HCT116 cells were transfected with ΔTBP7-Flag deletion mutant, harvested and immunoprecipitated with anti-TRAP1 antibodies as described in Materials and Methods.

Immunoprecipitates were separated by SDS-PAGE and immunoblotted with the indicated antibodies. No Ab, total cellular extracts incubated with A/G plus agarose beads without antibody; IP, immunoprecipitation with the corresponding antibodies. Three independent experiments were performed with similar results. Arrow indicates the ΔTBP7-Flag mutant band.

I) Ubiquitination levels upon transfection of ΔTBP7-Flag deletion mutant

Total lysates from HCT116 scrambled cells transfected with ΔTBP7-Flag mutant were subjected to immunoblot analysis with mouse monoclonal anti-Ubiquitin antibodies to detect total ubiquitination levels and with mouse monoclonal anti-HSP60 antibodies for the normalization of cell lysates. Three independent experiments were performed with similar results.

Figure 5: Control of intracellular protein stability and ubiquitination pattern of p18 Sorcin and F1ATPase

A) Pulse-chase analysis of total lysates of scrambled and sh-TRAP1 HCT116 cells. HCT116 cells were incubated in cysteine/methionine-free medium for 1 h followed by incubation in cysteine/methionine-free medium containing 50 μCi/mL ^{35}S-labeled cysteine/methionine (^{35}S Met/^{35}S Cys) for 1 h. After labelling, cells were washed once with culture medium containing 10-fold excess of unlabeled methionine and cysteine (5mM each) and incubated further in the same medium for the indicated times. Cells were collected at the indicated time points, and total lysates subjected to SDS-PAGE were analyzed by autoradiography.

B) Total lysates of scrambled and sh-TRAP1 HCT116 cells were subjected to SDS-PAGE and immunoblotted with rabbit polyclonal anti-Sorcin, mouse monoclonal anti-TRAP1, goat polyclonal anti-F1ATPase antibodies. The same filter was re-probed with mouse monoclonal anti-GAPDH antibodies for the normalization of cell lysates. Arrow indicates the mitochondrial 18kDa Sorcin isoform band.

C) Scrambled and sh-TRAP1 HCT116 clones were transfected with an expression vector containing the cDNA of p18 sorcin fused to C-Myc epitope at C-terminus (Sorcin-Myc) and treated with 1μM

MG132 for 24 h before harvesting. Lysates were immunoprecipitated with mouse monoclonal anti-Myc antibodies, and analyzed by immunoblot analysis with mouse monoclonal anti-Ubiquitin antibodies. The membrane was re-probed with anti-Myc antibody to control transfection efficiency.

D) Scrambled and sh-TRAP1 HCT116 clones were treated with 1μM MG132 for 24 h before harvesting, immunoprecipitated with anti-F1ATPase antibody, subjected to SDS-PAGE and immunoblotted with mouse monoclonal anti-Ubiquitin and goat polyclonal anti-F1ATPase antibodies. Three independent experiments were performed with similar results.

E) HCT116 cells were co-transfected with a Ub-HA vector and siRNA negative control (scramble), or with siRNAs specific for TBP7, treated with 1μM MG132 for 24 h before harvesting, immunoprecipitated with goat polyclonal anti-F1ATPase antibody, subjected to SDS-PAGE and immunoblotted with mouse monoclonal anti-Ubiquitin and goat polyclonal anti-F1ATPase antibodies. Three independent experiments were performed with similar results.

Figure 6: TRAP1, TBP7, F1ATPase and Sorcin expression in human colorectal carcinomas.

Total cell lysates from 4 human colorectal carcinomas (T) and the respective non-infiltrated peritumoral mucosas (M) were separated by SDS–PAGE and immunoblotted with rabbit polyclonal anti-Sorcin, mouse monoclonal anti-TRAP1, mouse monoclonal anti-TBP7, goat polyclonal anti-F1ATPase. The same filter was re-probed with mouse monoclonal anti-GAPDH antibodies for the normalization of cell lysates. Case numbers are refereed to Supplementary Figure 1.

Figure 7: Crosstalk between ER and mitochondria and mitochondrial protein quality control.

TRAP1 form a supramolecular complex with TBP7 on the outside of the ER, in a cellular compartment of tight ER-mitochondria contact sites, where proteasomes are also present. This TRAP1/TBP7 complex is involved in the control of protein stability and intracellular protein ubiquitination of mitochondria-destined proteins. These two proteins, each with independent but

related functions, help to judge whether a protein can be repaired and reach the final mitochondrial destination or, if damaged, needs to be degraded through the ubiquitin-proteasome system.

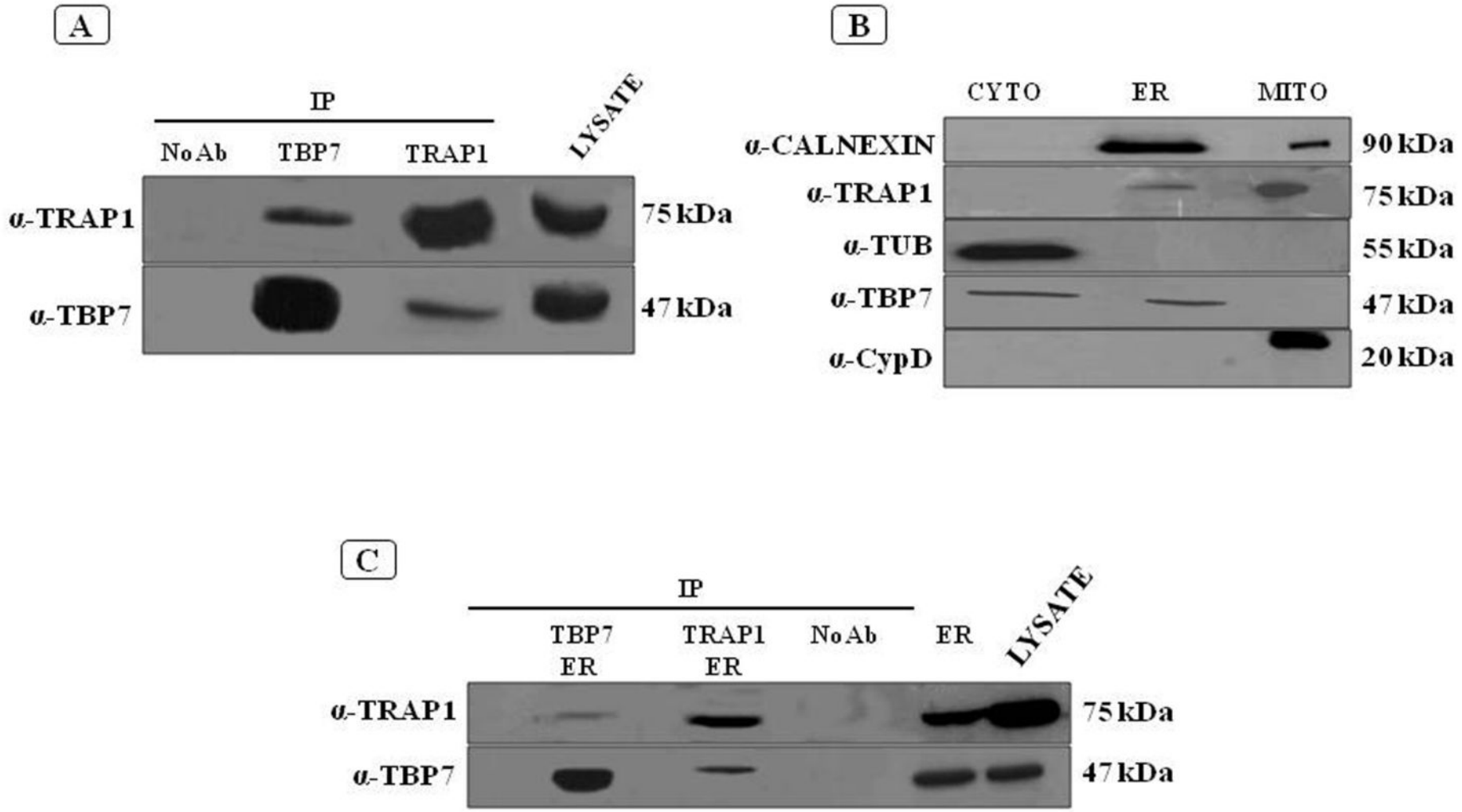
A
IP
NoAb
TBP7
TRAP1
LYSATE
α-TRAP1
α-TBP7
75kDa
47kDa
B
CYTO
ER
MITO
α-CALNEXIN
α-TRAP1
α-TUB
α-TBP7
α-CypD
90kDa
75kDa
55kDa
47kDa
20kDa
C
IP
TBP7 ER
TRAP1 ER
NoAb
ER
LYSATE
α-TRAP1
α-TBP7
75kDa
47kDa

Figure 1

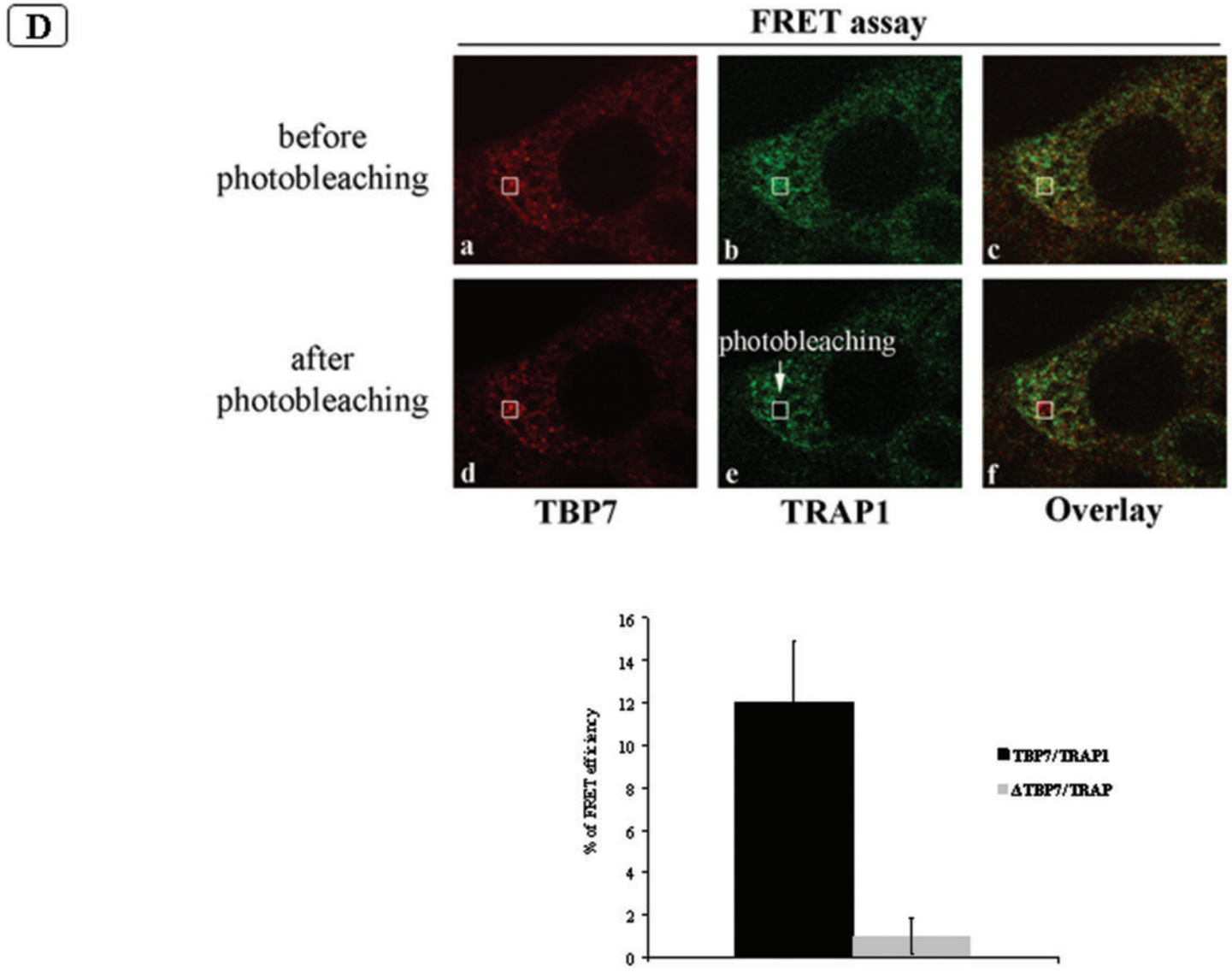
D
FRET assay
before photobleaching
after photobleaching
a
b
c
d
e
f
photobleaching
TBP7
TRAP1
Overlay
% of FRET efficiency
16
14
12
10
8
6
4
2
0
TBP7/TRAP1
ΔTBP7/TRAP

Figure 1

E

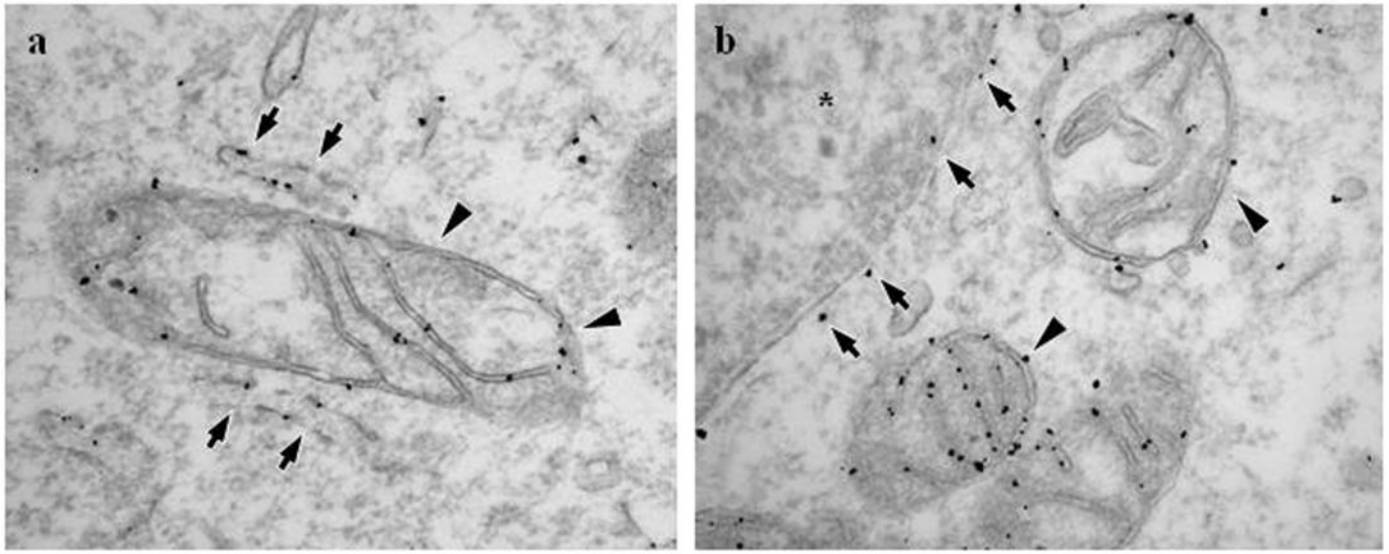

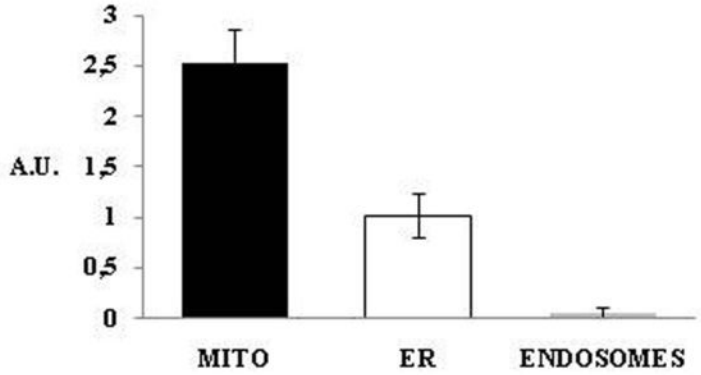

Figure 1

F

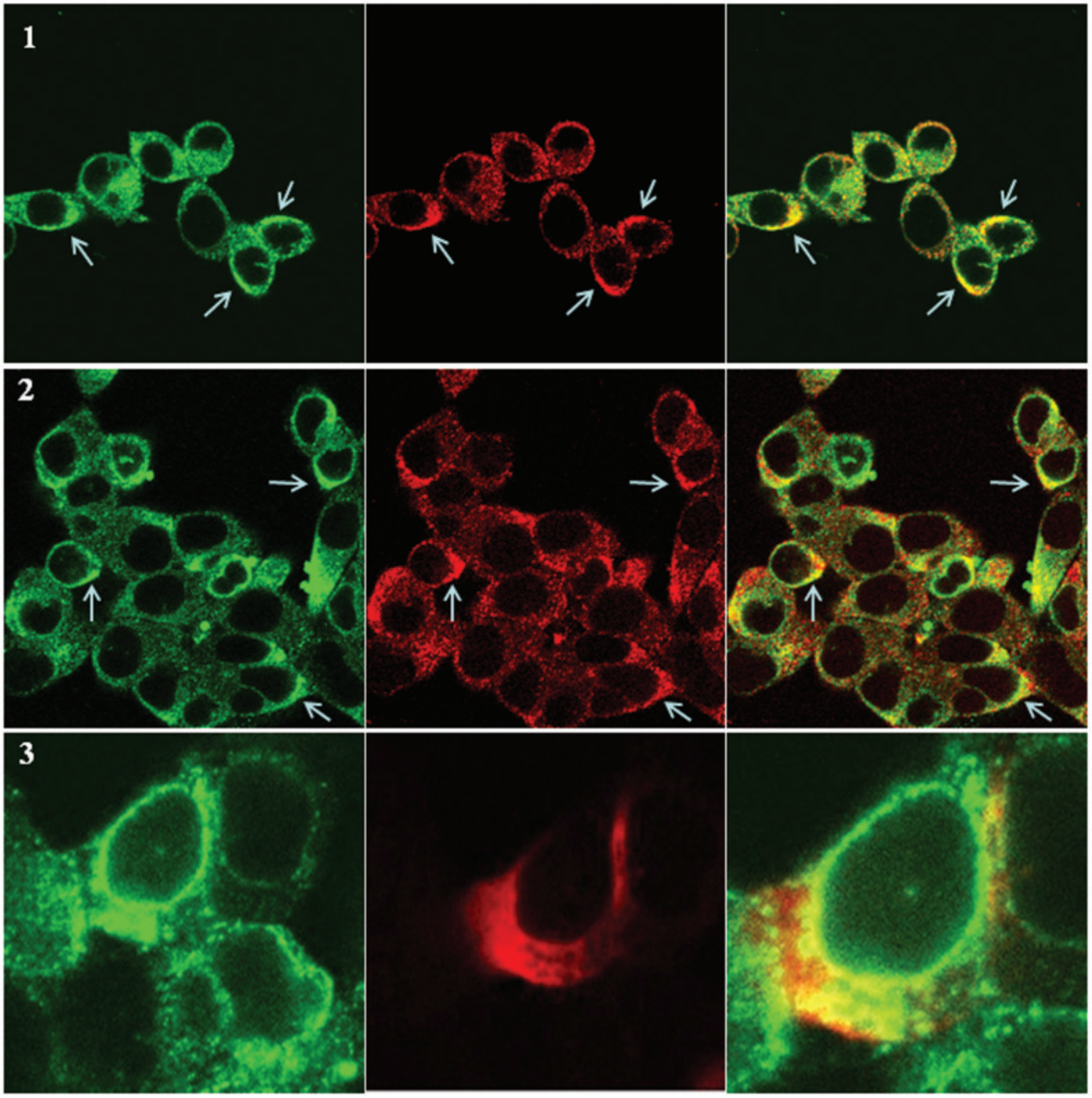

Figure 1

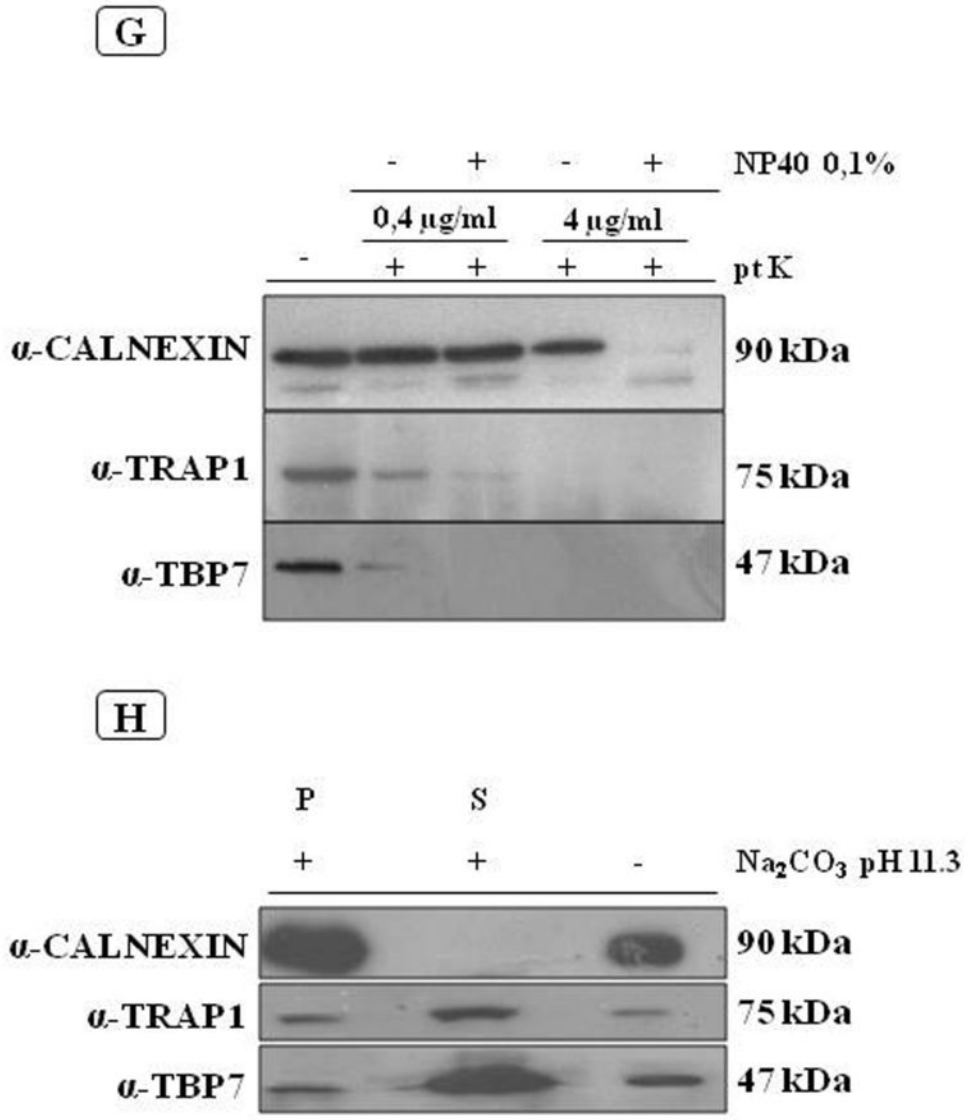
G
- + - + NP40 0,1%
0,4 µg/ml
4 µg/ml
- + + + + ptK
α-CALNEXIN
90 kDa
α-TRAP1
75 kDa
α-TBP7
47 kDa
H
P
S
+ + - Na2CO3 pH 11.3
α-CALNEXIN
90 kDa
α-TRAP1
75 kDa
α-TBP7
47 kDa

Figure 1

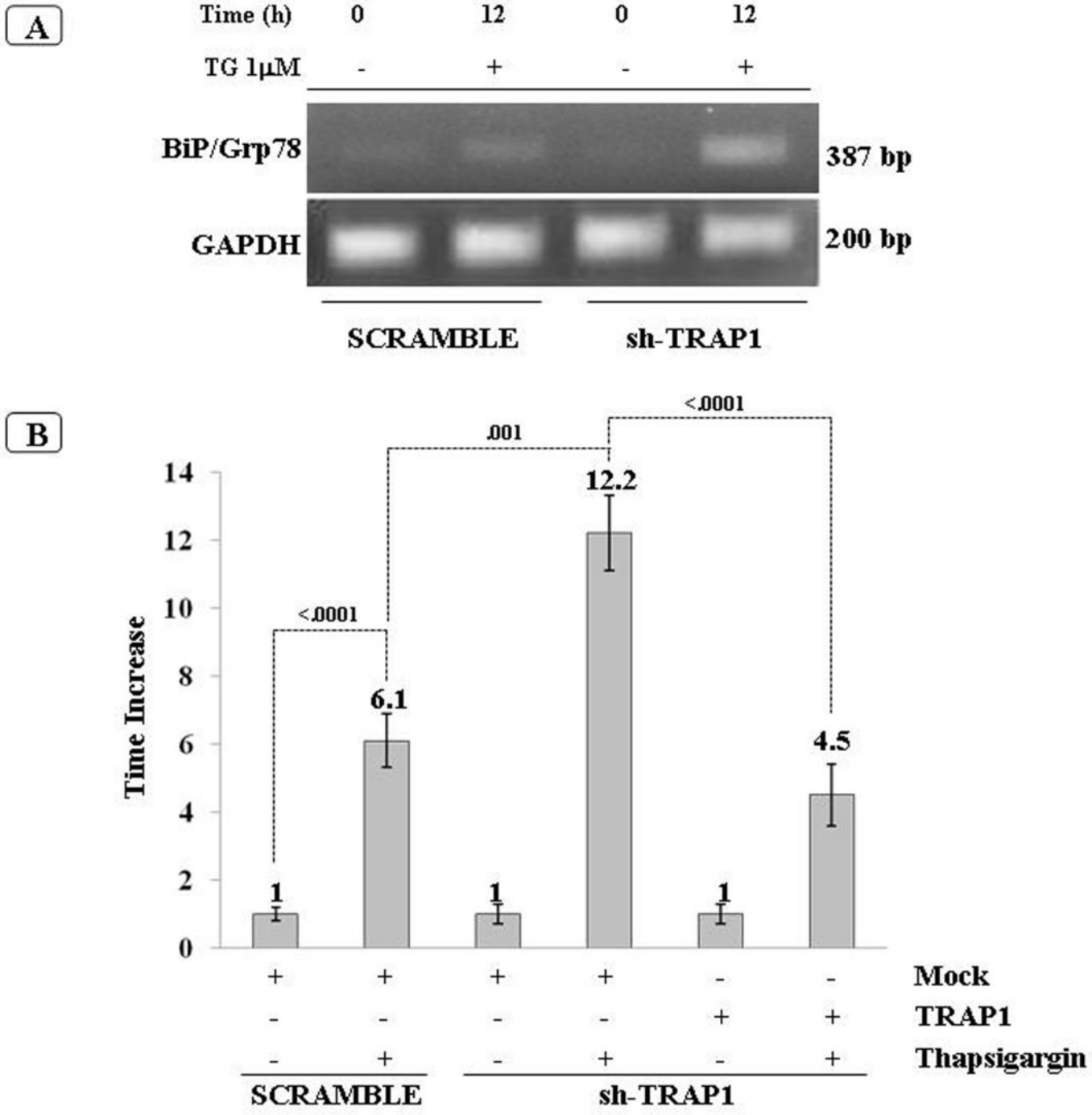
A
Time (h)
0
12
0
12
TG 1μM
-
+
-
+
BiP/Grp78
387 bp
GAPDH
200 bp
SCRAMBLE
sh-TRAP1
B
<.0001
.001
<.0001
12.2
6.1
4.5
1
1
1
Time Increase
14
12
10
8
6
4
2
0
+
+
+
+
-
-
Mock
-
-
-
-
+
+
TRAP1
-
+
-
+
-
+
Thapsigargin
SCRAMBLE
sh-TRAP1

Figure 2

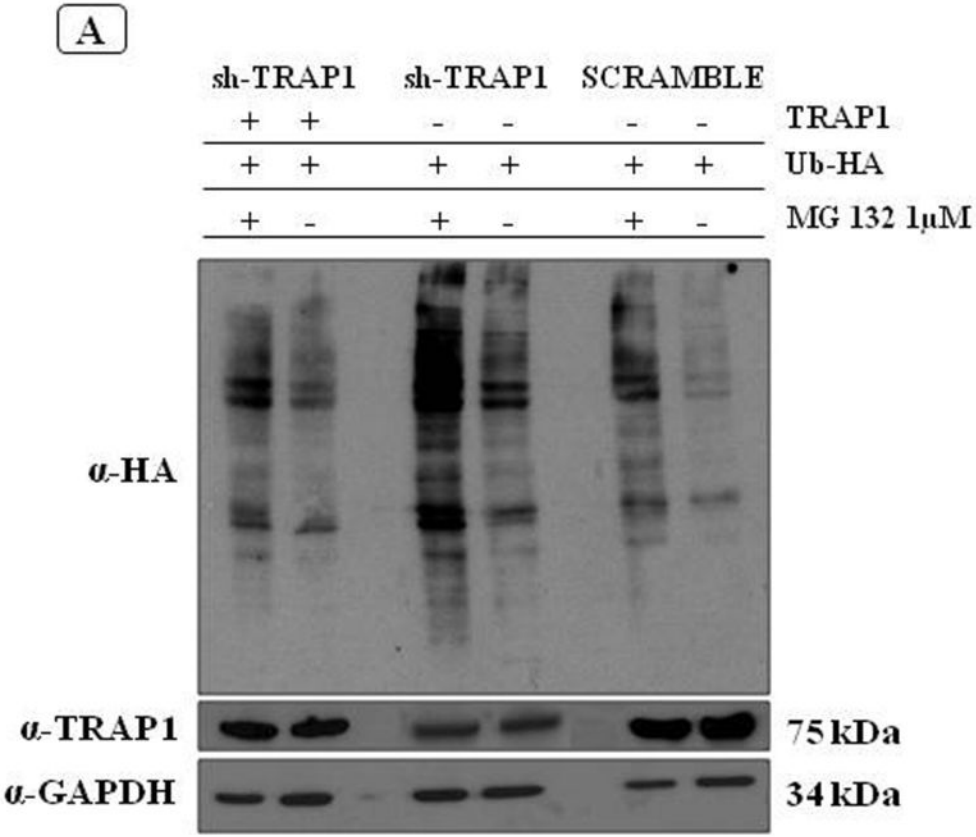
A
sh-TRAP1
sh-TRAP1
SCRAMBLE
+ + - - - - TRAP1
+ + + + + + Ub-HA
+ - + - + - MG 132 1μM
α-HA
α-TRAP1
75 kDa
α-GAPDH
34 kDa

Figure 3

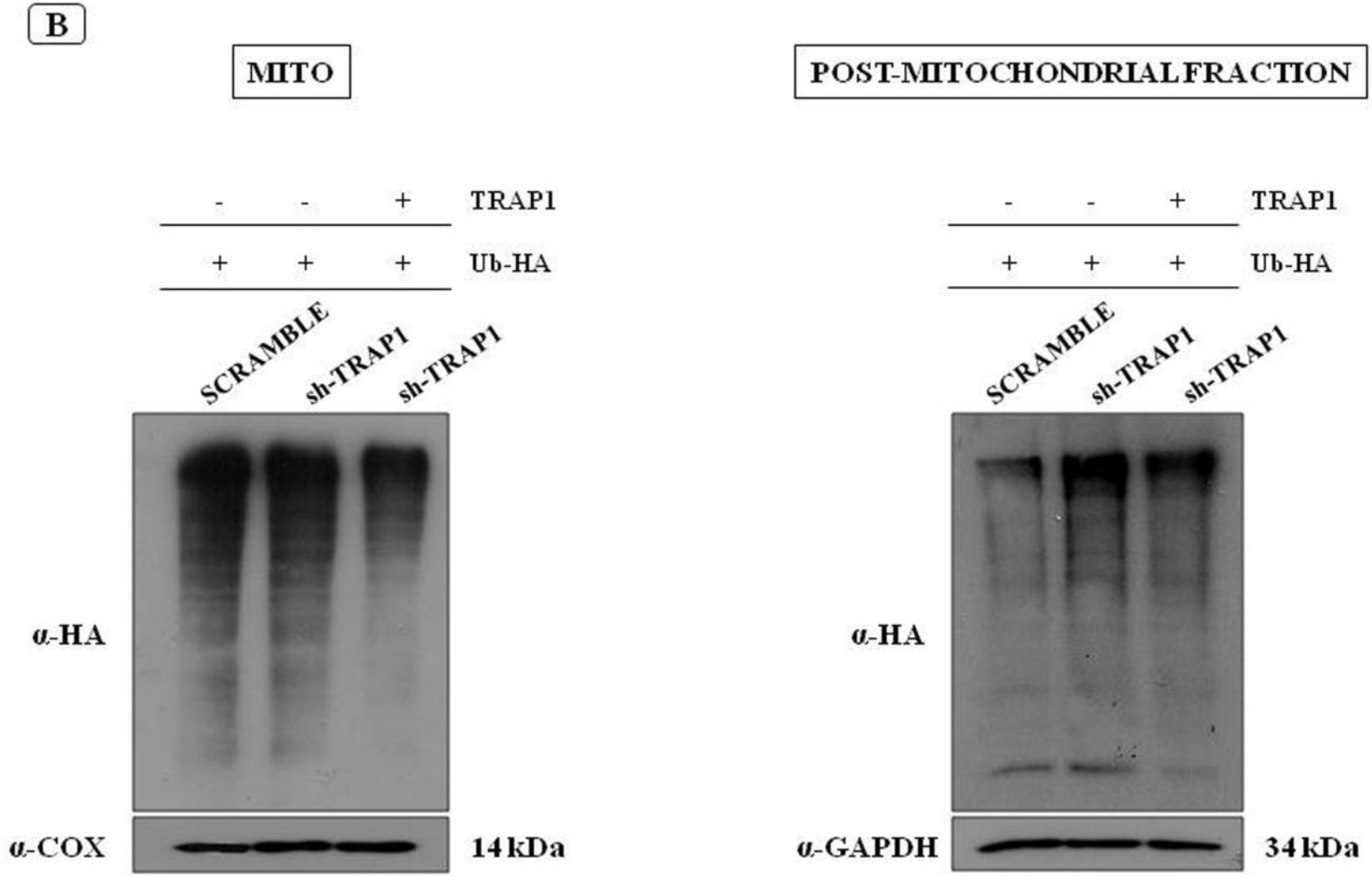
B
MITO
POST-MITOCHONDRIAL FRACTION
- - + TRAP1
+ + + Ub-HA
SCRAMBLE
sh-TRAP1
sh-TRAP1
α-HA
α-COX
14 kDa
α-GAPDH
34 kDa

Figure 3

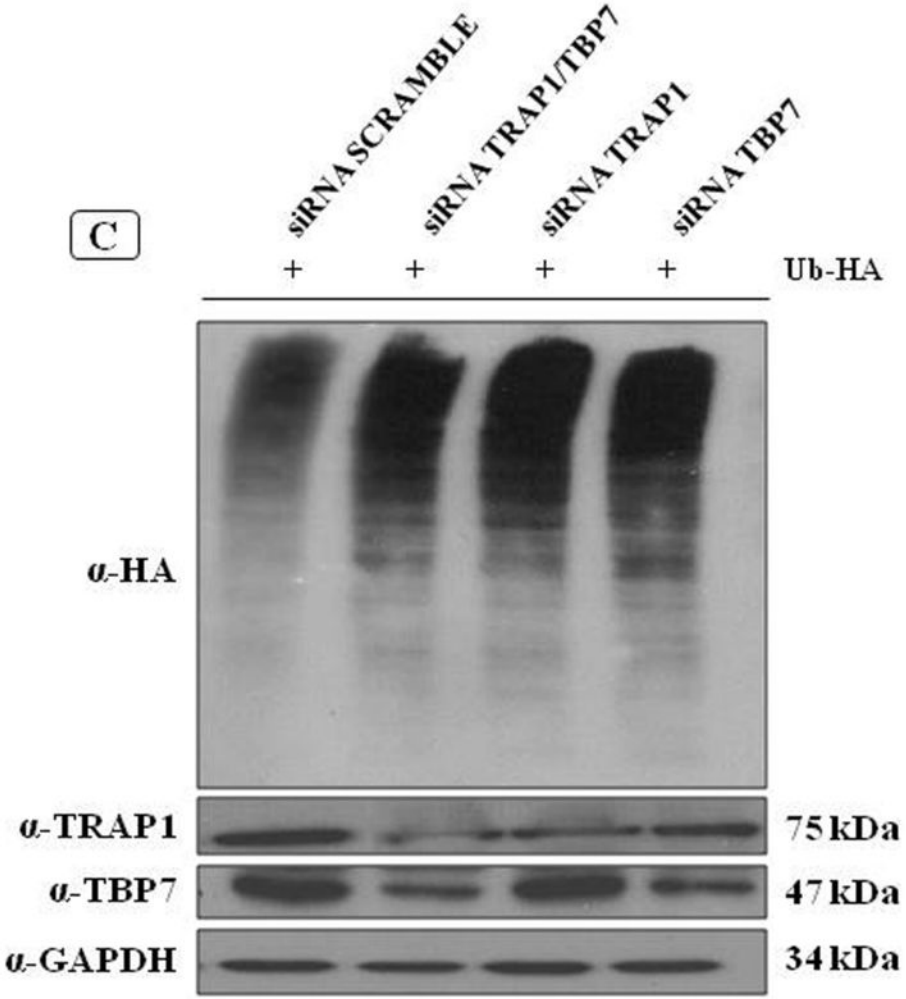
C
siRNA SCRAMBLE
siRNA TRAP1/TBP7
siRNA TRAP1
siRNA TBP7
+ + + + Ub-HA
α-HA
α-TRAP1
α-TBP7
α-GAPDH
75 kDa
47 kDa
34 kDa

Figure 3

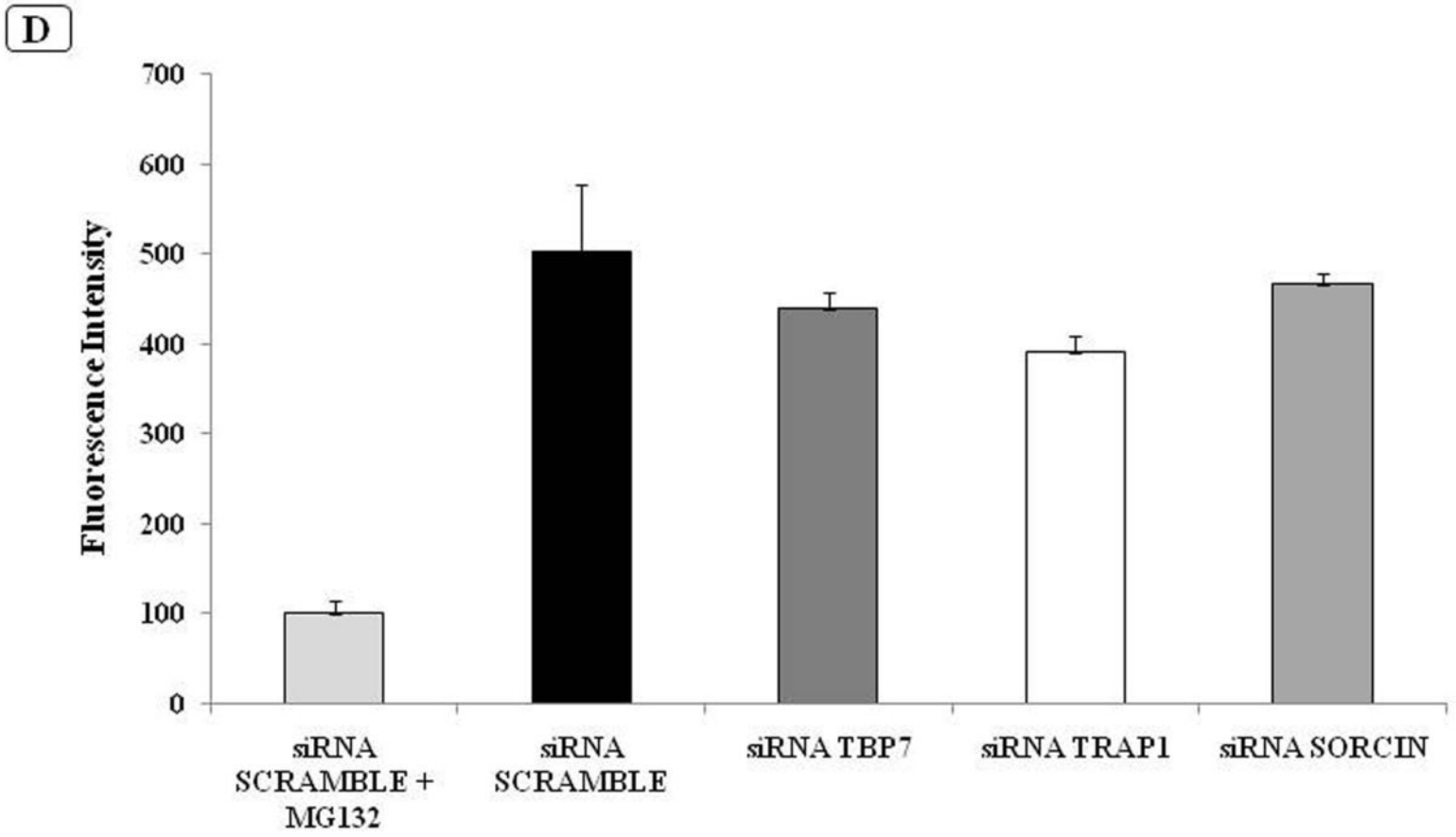
D
Fluorescence Intensity
700
600
500
400
300
200
100
0
siRNA SCRAMBLE + MG132
siRNA SCRAMBLE
siRNA TBP7
siRNA TRAP1
siRNA SORCIN

Figure 3

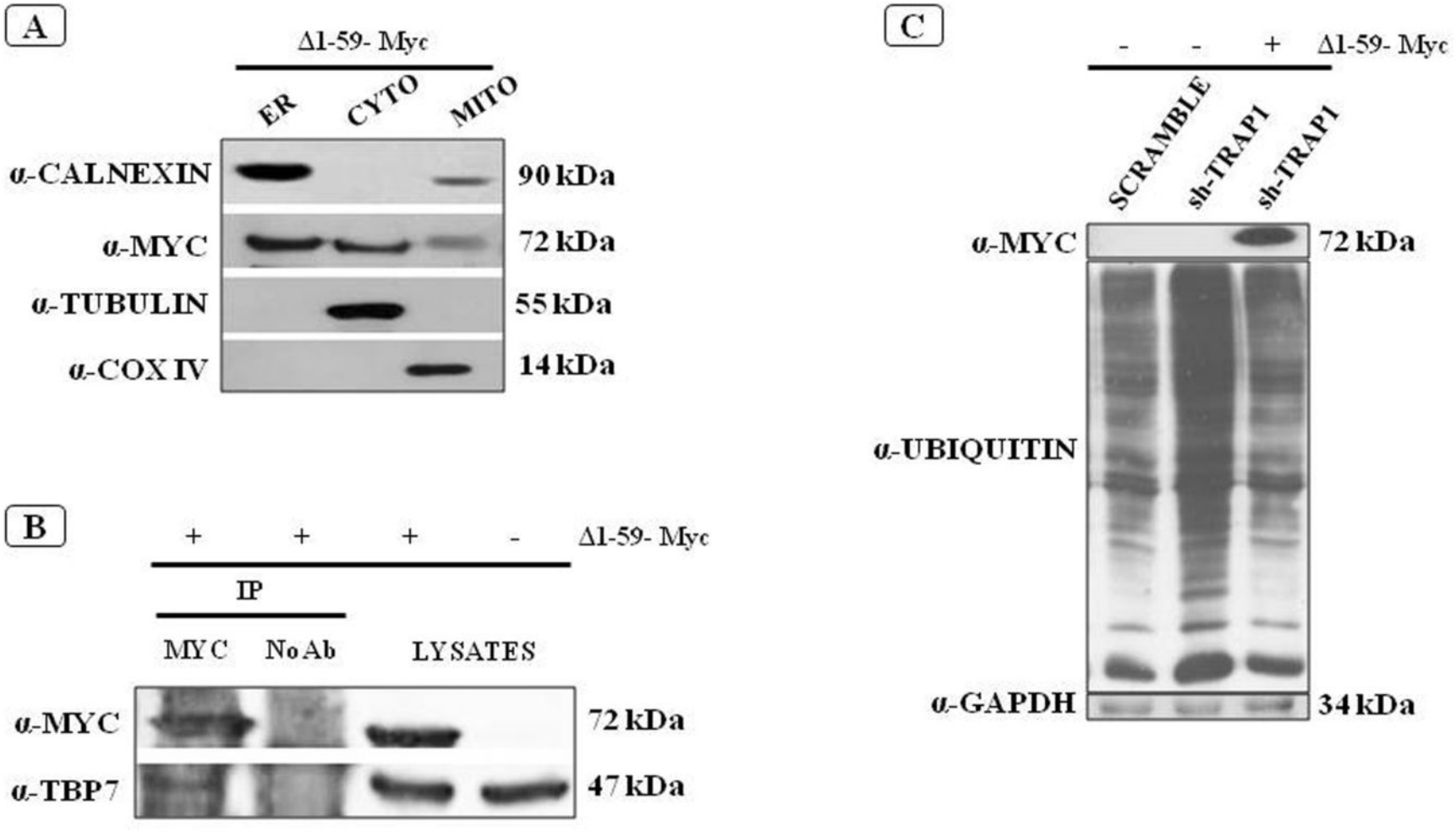
A
Δ1-59- Myc
ER
CYTO
MITO
α-CALNEXIN
90 kDa
α-MYC
72 kDa
α-TUBULIN
55 kDa
α-COX IV
14 kDa
B
+
+
+
-
Δ1-59- Myc
IP
MYC
No Ab
LYSATES
α-MYC
72 kDa
α-TBP7
47 kDa
C
-
-
+
Δ1-59- Myc
SCRAMBLE
sh-TRAP1
sh-TRAP1
α-MYC
72 kDa
α-UBIQUITIN
α-GAPDH
34 kDa

Figure 4

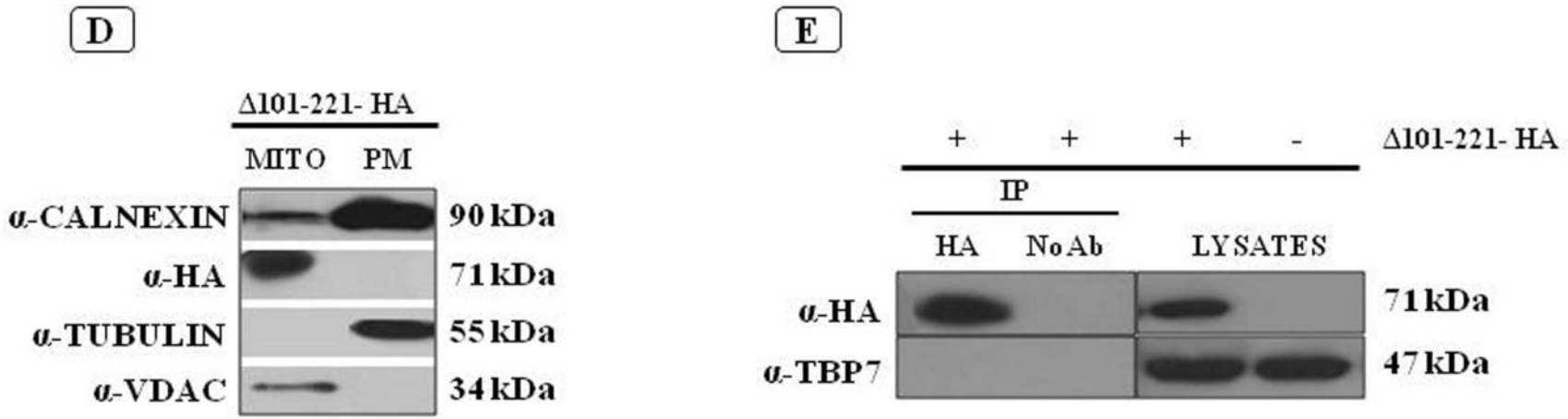
D
Δ101-221- HA
MITO
PM
α-CALNEXIN
90 kDa
α-HA
71 kDa
α-TUBULIN
55 kDa
α-VDAC
34 kDa
E
+
+
+
-
Δ101-221- HA
IP
HA
NoAb
LYSATES
α-HA
71 kDa
α-TBP7
47 kDa

Figure 4

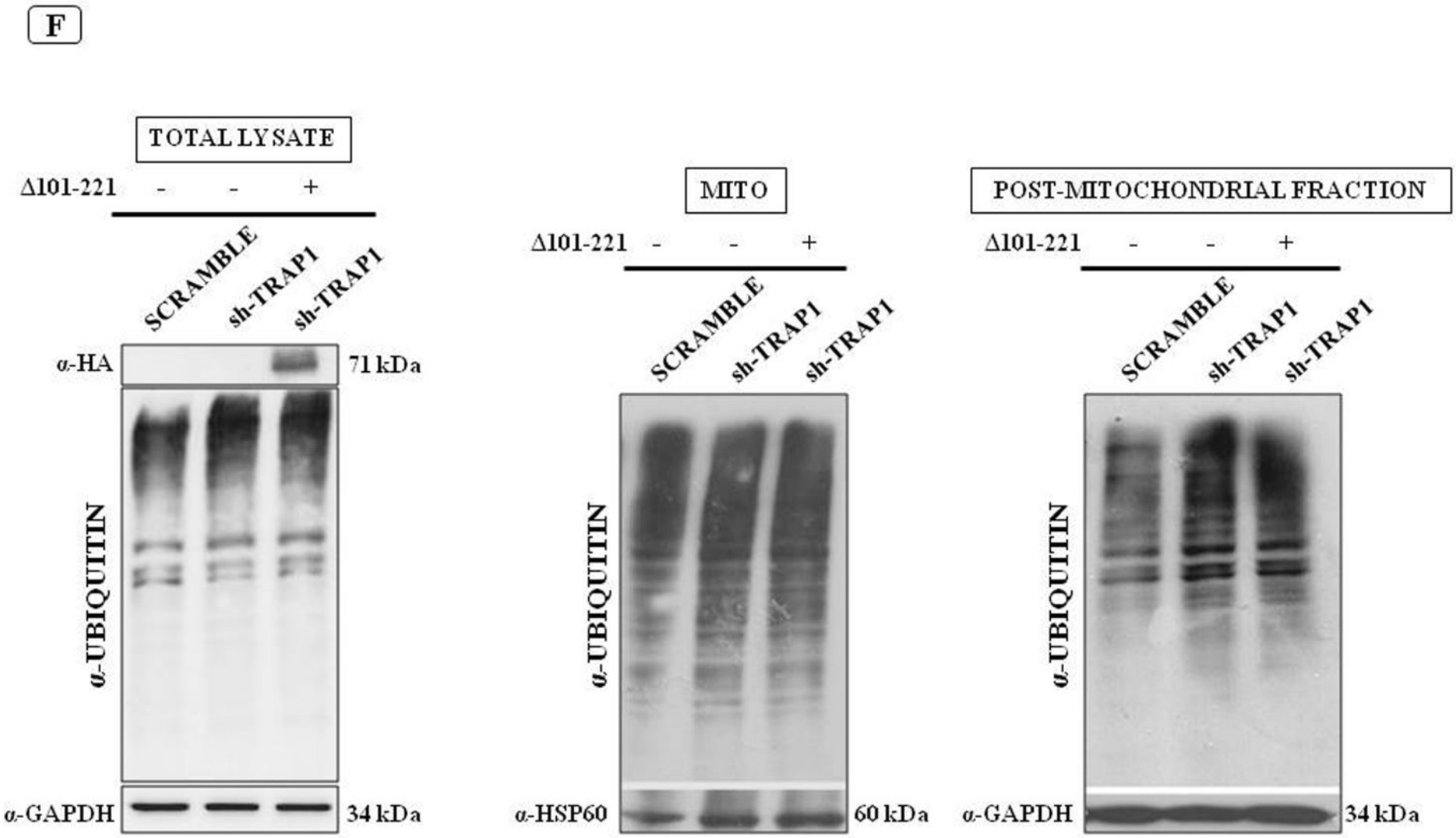
F
TOTAL LYSATE
Δ101-221 - - +
SCRAMBLE
sh-TRAP1
sh-TRAP1
α-HA
71 kDa
α-UBIQUITIN
α-GAPDH
34 kDa
MITO
Δ101-221 - - +
SCRAMBLE
sh-TRAP1
sh-TRAP1
α-UBIQUITIN
α-HSP60
60 kDa
POST-MITOCHONDRIAL FRACTION
Δ101-221 - - +
SCRAMBLE
sh-TRAP1
sh-TRAP1
α-UBIQUITIN
α-GAPDH
34 kDa

Figure 4

G

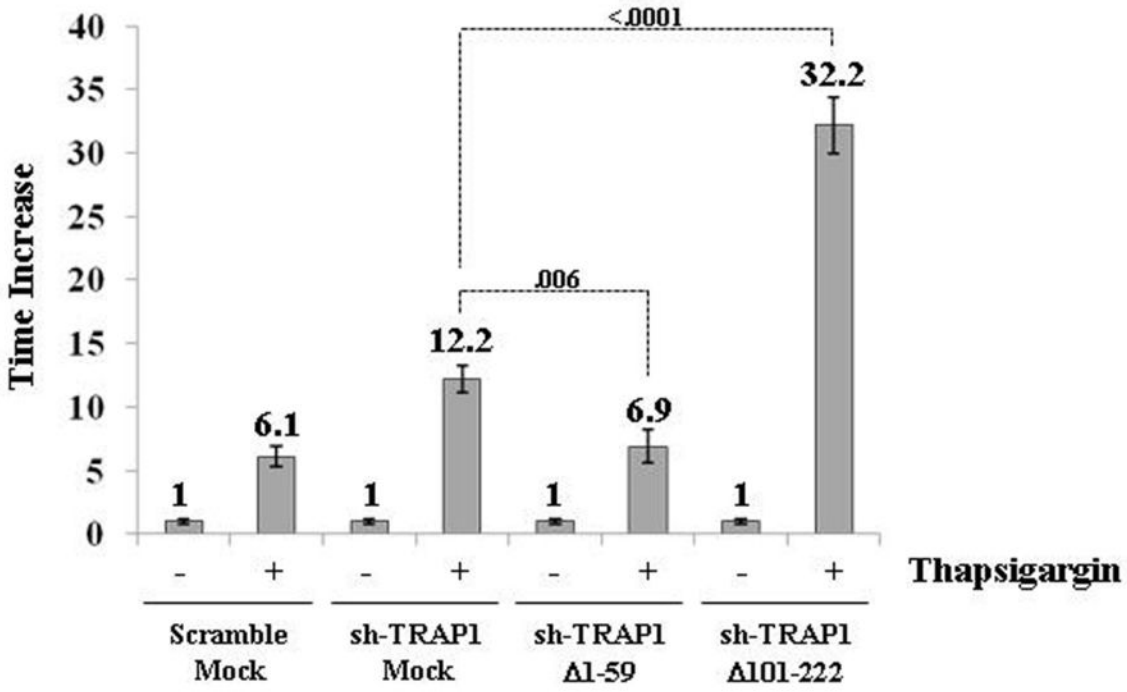
Time Increase
40
35
30
25
20
15
10
5
0
<.0001
.006
32.2
12.2
6.9
6.1
1
1
1
1
- + - + - + - +
Thapsigargin
Scramble Mock
sh-TRAP1 Mock
sh-TRAP1 Δ1-59
sh-TRAP1 Δ101-222

Figure 4

H

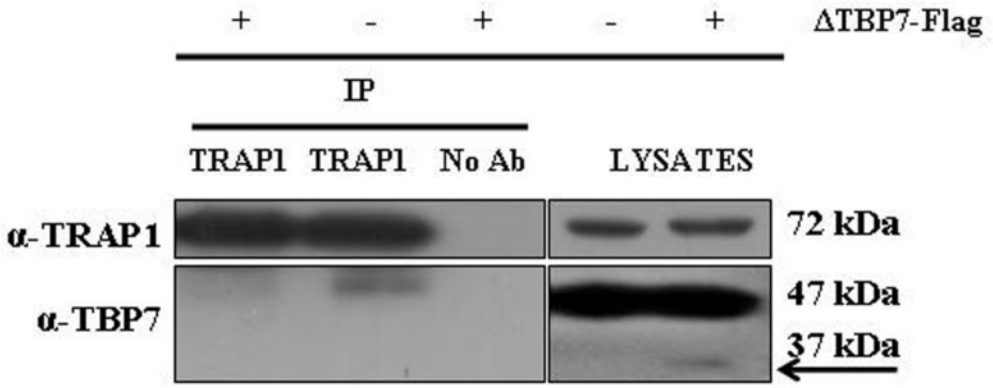
+ - + - + ΔTBP7-Flag
IP
TRAP1 TRAP1 No Ab LYSATES
α-TRAP1
α-TBP7
72 kDa
47 kDa
37 kDa

I

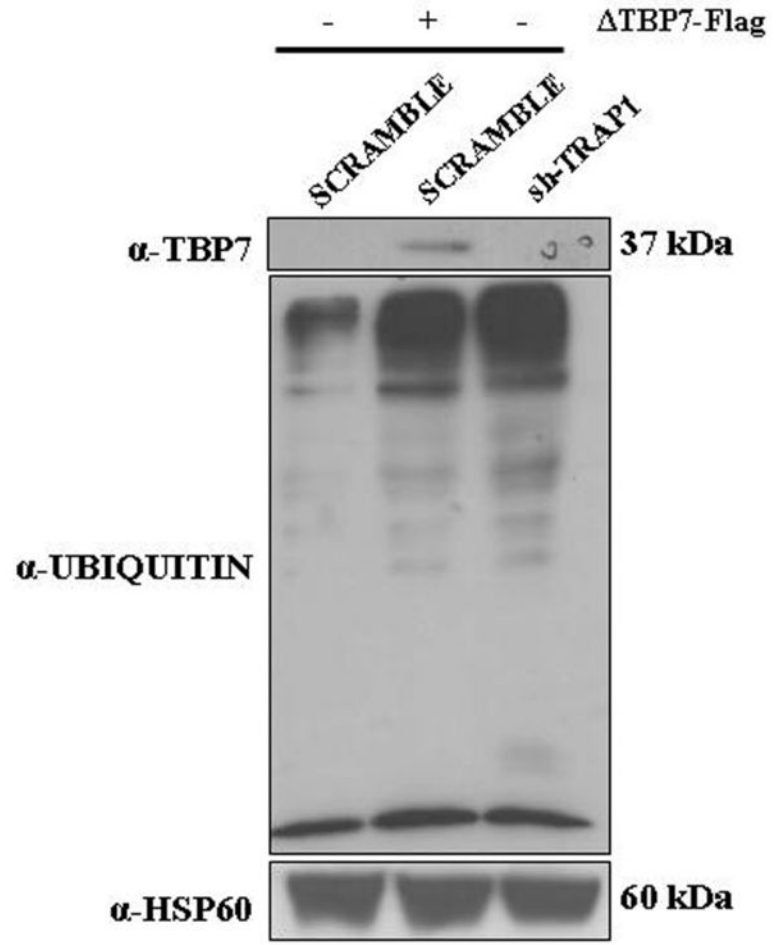
- + - ΔTBP7-Flag
SCRAMBLE SCRAMBLE sh-TRAP1
α-TBP7
37 kDa
α-UBIQUITIN
α-HSP60
60 kDa

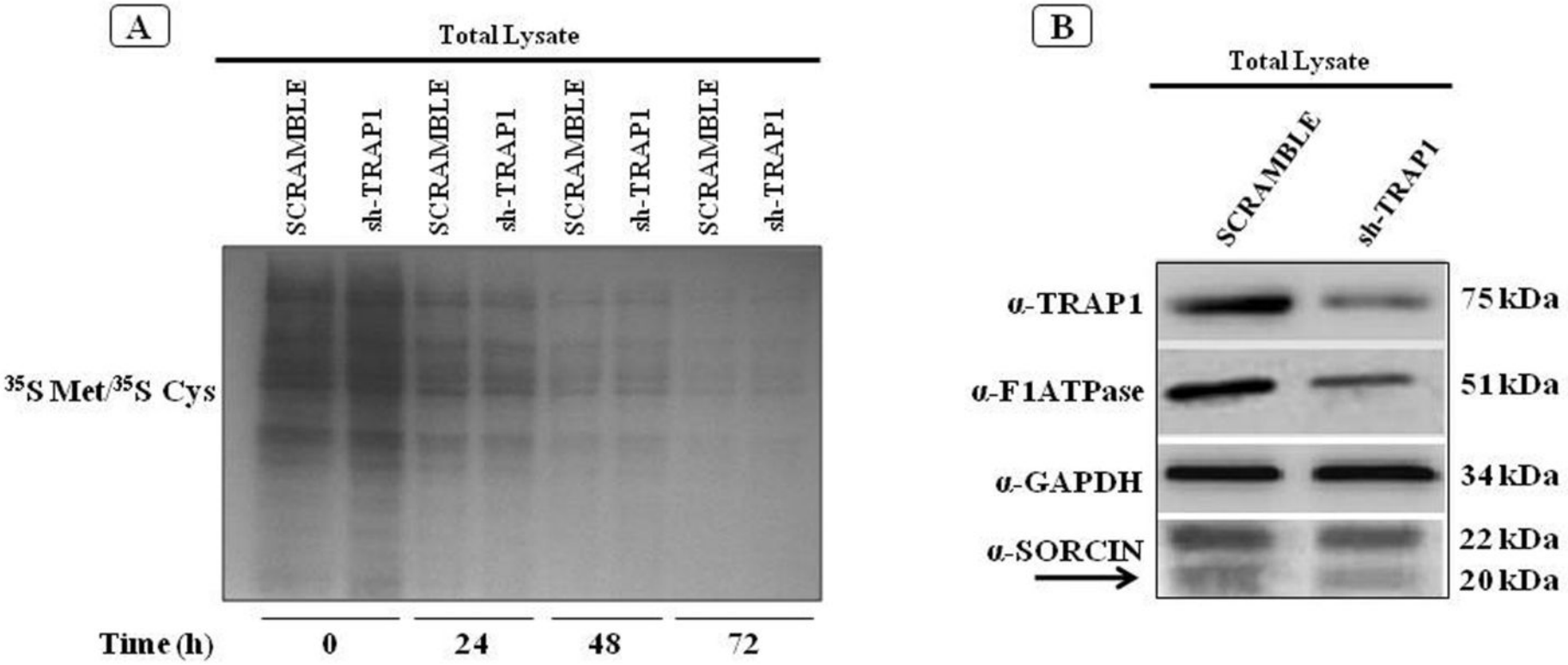
A
Total Lysate
SCRAMBLE
sh-TRAP1
SCRAMBLE
sh-TRAP1
SCRAMBLE
sh-TRAP1
SCRAMBLE
sh-TRAP1
35S Met/35S Cys
Time (h)
0
24
48
72
B
Total Lysate
SCRAMBLE
sh-TRAP1
α-TRAP1
75 kDa
α-F1ATPase
51 kDa
α-GAPDH
34 kDa
α-SORCIN
22 kDa
20 kDa

Figure 5

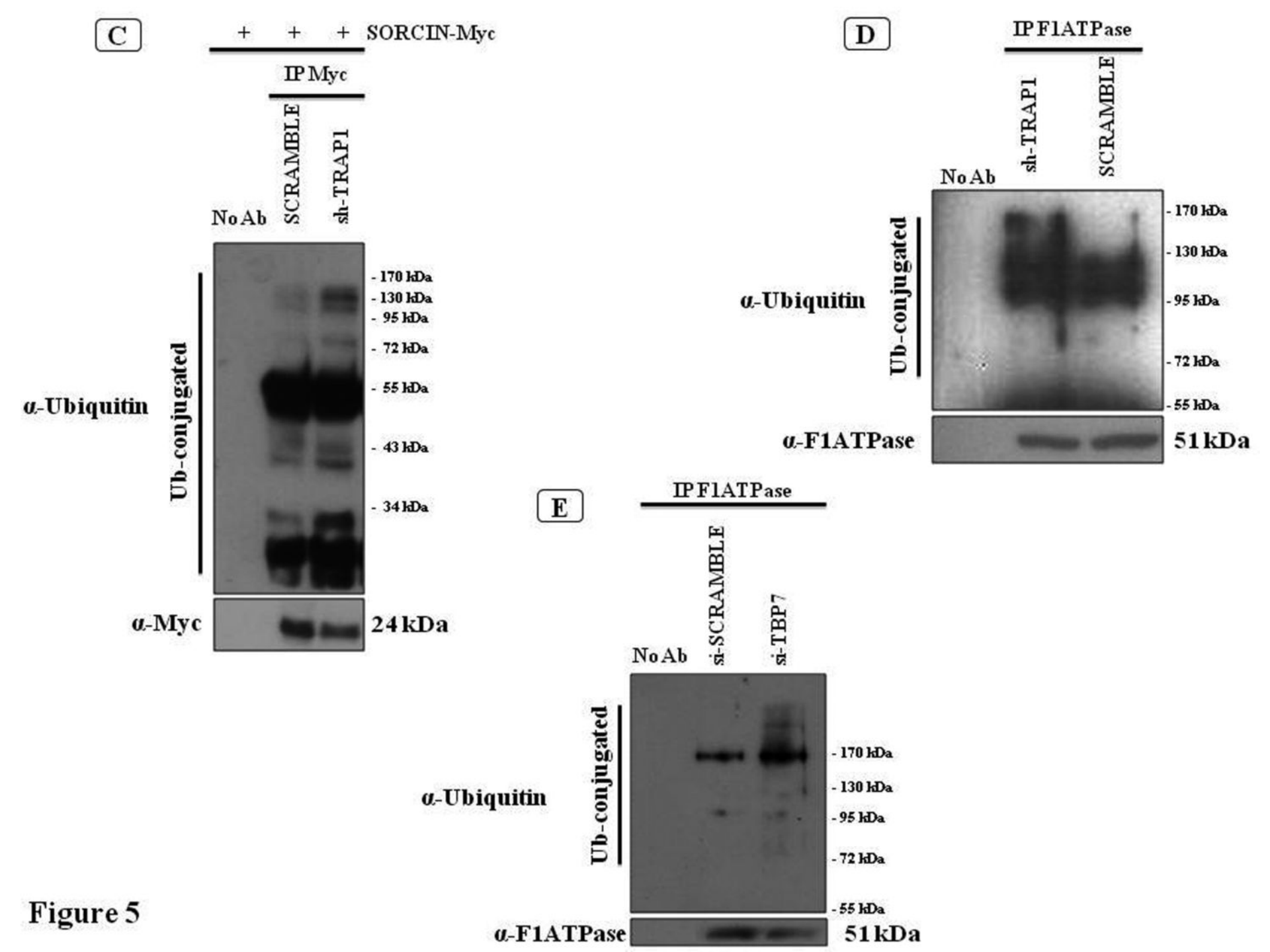
C
+ + + SORCIN-Myc
IP Myc
SCRAMBLE
sh-TRAP1
No Ab
Ub-conjugated
α-Ubiquitin
- 170 kDa
- 130 kDa
- 95 kDa
- 72 kDa
- 55 kDa
- 43 kDa
- 34 kDa
α-Myc
24 kDa
D
IP F1ATPase
sh-TRAP1
SCRAMBLE
No Ab
α-Ubiquitin
Ub-conjugated
- 170 kDa
- 130 kDa
- 95 kDa
- 72 kDa
- 55 kDa
α-F1ATPase
51 kDa
E
IP F1ATPase
si-SCRAMBLE
si-TBP7
No Ab
α-Ubiquitin
Ub-conjugated
- 170 kDa
- 130 kDa
- 95 kDa
- 72 kDa
- 55 kDa
α-F1ATPase
51 kDa

Figure 5

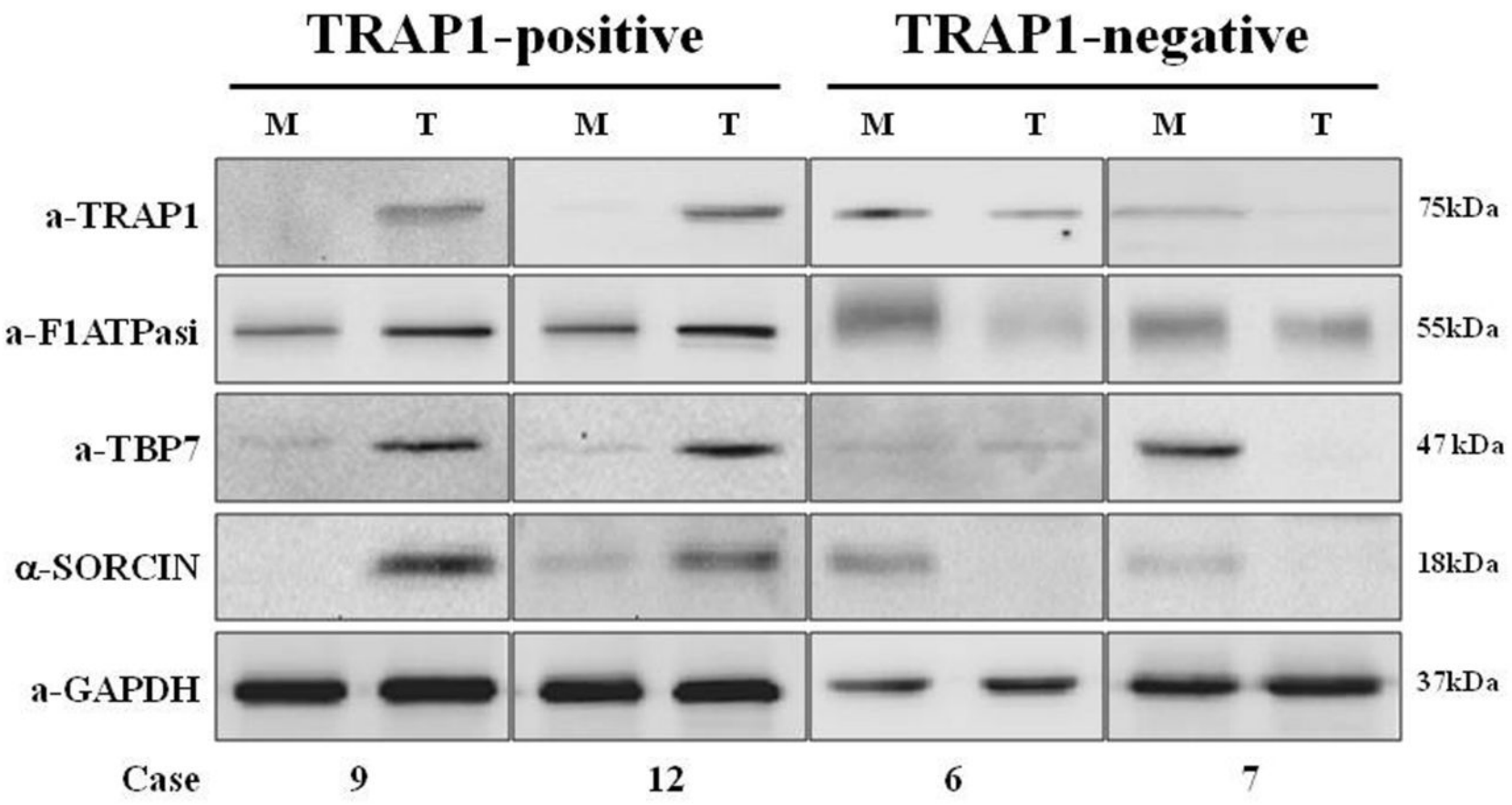
TRAP1-positive
TRAP1-negative
M
T
M
T
M
T
M
T
a-TRAP1
a-F1ATPasi
a-TBP7
α-SORCIN
a-GAPDH
75kDa
55kDa
47kDa
18kDa
37kDa
Case
9
12
6
7

Figure 6

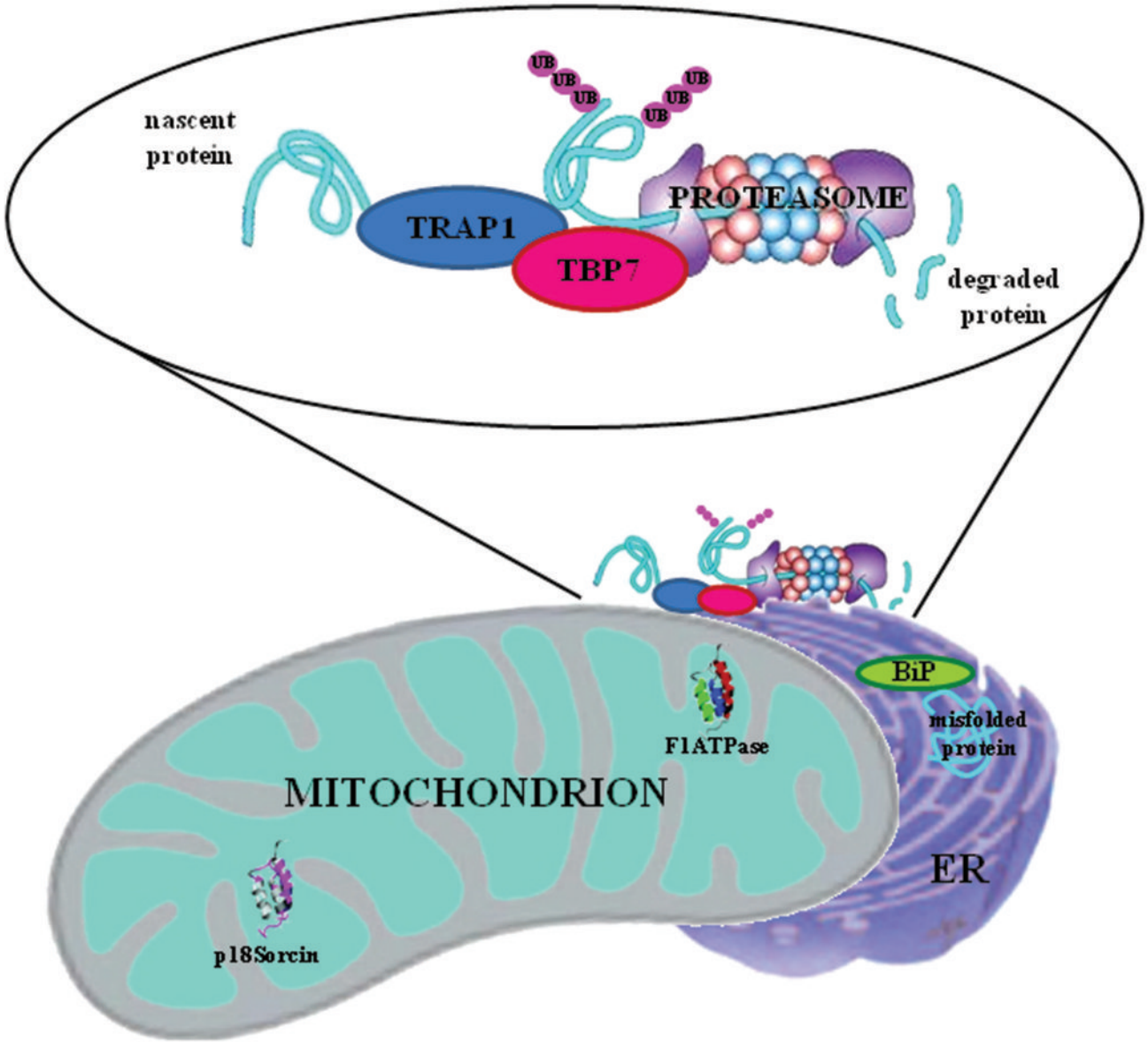
UB
UB
UB
UB
UB
UB
nascent
protein
TRAP1
TBP7
PROTEASOME
degraded
protein
BiP
misfolded
protein
F1ATPase
MITOCHONDRION
ER
p18Sorcin

Figure 7

Table 1. Rates of apoptotic cell death in colorectal carcinoma HCT116 cells treated with 1μM thapsigargin (TG) for 24h or with 10μM oxaliplatin (l-OHP) for 48 h upon transient (siRNA) or stable (shRNA) down-regulation of TRAP1 or TBP7. Ratios are calculated between rates of apoptosis in drug- and vehicle-treated cells. P-values indicate the statistical significance between the ratios of apoptosis in siRNA-transfected cells and the respective scramble controls.

	Apoptosis (%±SD)	**Ratio (±SD)**	**p-value**
	Vehicle		
Scramble			
Vehicle	3.5±0.3		
TG	5.0±0.2	1.4±0.2	
l-OHP	11.2±0.4	3.2±0.4	
siRNA TRAP1			
Vehicle	4.7±0.2		
TG	21.5±.0.4	4.6±0.3	<0.0001
l-OHP	55.5±0.6	11.8±0.7	<0.0001
shRNA TRAP1			
Vehicle	3.5±0.4		
TG	24.2±.0.5	6.9±1.1	0.001
l-OHP	31.8±0.4	9.1±1.3	0.002
siRNA TBP7			
Vehicle	5.2±0.2		
TG	15.7±0.3	3.0±0.2	<0.0001
l-OHP	55.1±0.6	10.6±0.5	<0.0001